International Journal of Pharmaceutics xxx (xxxx) xxx–xxx

Contents lists available at ScienceDirect

International Journal of Pharmaceutics

journal homepage: www.elsevier.com/locate/ijpharm

BioMEMS for biosensors and closed-loop drug delivery

Joel Coffel, Eric Nuxoll*

Department of Chemical and Biochemical Engineering, 4133 Seamans Center for the Engineering Arts & Sciences, University of Iowa, Iowa City, IA 52242, USA

ARTICLE INFO

Keywords:
BioMEMS
Biosensors
Signal transduction
Drug delivery
Biofouling

ABSTRACT

The efficacy of pharmaceutical treatments can be greatly enhanced by physiological feedback from the patient using biosensors, though this is often invasive or infeasible. By adapting microelectromechanical systems (MEMS) technology to miniaturize such biosensors, previously inaccessible signals can be obtained, often from inside the patient. This is enabled by the device's extremely small footprint which minimizes both power consumption and implantation trauma, as well as the transport time for chemical analytes, in turn decreasing the sensor's response time. MEMS fabrication also allows mass production which can be easily scaled without sacrificing its high reproducibility and reliability, and allows seamless integration with control circuitry and telemetry which is already produced using the same materials and fabrication steps. By integrating these systems with drug delivery devices, many of which are also MEMS-based, closed loop drug delivery can be achieved. This paper surveys the types of signal transduction devices available for biosensing—primarily electrochemical, optical, and mechanical—looking at their implementation *via* MEMS technology. The impact of MEMS technology on the challenges of biosensor development, particularly safety, power consumption, degradation, fouling, and foreign body response, are also discussed.

1. Introduction

Physiological measurements to optimize drug delivery can be inconvenient, invasive, or even painful, limiting their frequency and therefore utility. One strategy for enhancing the frequency and accuracy of these measurements is incorporation of microelectromechanical systems (MEMS) technology (Madou, 2011; Tilli et al., 2015). In general, MEMS are defined by their small (submillimeter) length scale and their top-down fabrication techniques, where features are precisely machined from larger starting materials, as opposed to, for instance, self-assembly from smaller components based on their physicochemical interactions (Siegel et al., 2009). The advantages which biologically-oriented MEMS (BioMEMS) technology (Badilescu and Muthukumaran, 2011; Bashir and Wereley, 2006; Folch, 2012) can impart on biosensing, the ways in which it is being incorporated, and the challenges it must still overcome are the topic of this mini-review.

MEMS technology has been developed most extensively for the semiconductor industry, where machining tens of billions transistors into precisely aligned, interconnected arrays with no defects on a few square centimeters of silicon has become standard (Courtland, 2017). This is achieved by selectively processing parts of the silicon surface through a polymer stencil which protects the rest of the surface. The exposed surface may be etched away, chemically modified (doped), or covered with other materials (metals, insulators, *etc.*) while the protected surface is not. The stencil's features may be cut sequentially by a laser, an electron beam, or even a mechanical stylus, but most often they are all formed simultaneously in a photosensitive polymer by shining light through a mask onto it, selectively stabilizing or degrading the polymer in regions corresponding to the stencil features (photolithography). Once the less-stable material is washed away, the polymer stencil remains. This process may be repeated dozens of times, each with a different etching, doping, or deposition process, to reliably build micron- or nanometer-scale devices in quantities limited only by the size and number of wafers processed.

This approach to biosensor construction offers several potential advantages over conventional fabrication routes: First, the extremely small size of the systems permits applications which would be infeasible at larger length scales; for instance, sensing elements can be inserted in otherwise inaccessible locations. For measurements involving diffusive transport, the lag time decreases with the square of the transport length, strongly decreasing with device size. Smaller devices typically have lower power requirements and consume sacrificial chemicals at a slower rate, increasing potential device lifetime. Second, the fabrication processes are well-established and highly scalable, allowing rapid mass production of devices with extremely high reliability. Third, biosensors manufactured using MEMS processes and materials are particularly well-suited to integration with other MEMS devices, such as computer controls, wireless telemetry, and drug delivery modules.

* Corresponding author.
E-mail address: eric-nuxoll@uiowa.edu (E. Nuxoll).

https://doi.org/10.1016/j.ijpharm.2018.01.030
Received 9 September 2017; Received in revised form 10 January 2018; Accepted 14 January 2018

Already, BioMEMS technologies are permeating the development of drug delivery devices (Hilt and Peppas, 2005; Nuxoll, 2013), from microneedles for painless transdermal or intradermal delivery of biologics (Bhatnagar et al., 2017; Kim et al., 2012; Larraneta et al., 2016) to implanted microreservoir arrays delivering bone growth hormones (Farra et al., 2012). By integrating these delivery systems with computer control systems and biosensors, closed-loop drug delivery therapies can be achieved. In fact, some of the same simple devices used to transduce a physiological signal for reporting (*i.e.*, for biosensors) may also be used to transduce a signal for chemical release (*i.e.*, for drug delivery). The next section will survey these transduction devices by signal type, including electrochemical, optical, and mechanical transducers. The subsequent section will review recent progress in interfacing BioMEMS sensors with the body. Corrosion, fouling, and especially the foreign body response pose larger challenges to biosensors than to drug delivery systems. Though biosensors already comprise a 15 billion USD market with anticipated 9% annual growth (MarketsandMarkets, 2017; P&S Market Research, 2016), overcoming these challenges would allow permanent integration of biosensors in the body and expand their role in medicine enormously.

2. Signal transduction

The common function of all biosensors is transduction of a physiological signal, for instance a chemical analyte concentration, to a transmittable signal, typically electrical. Most of these transduction processes can be placed in one of three categories: electrochemical transduction where the analyte concentration directly causes a change in the potential, impedence, charge accumulation, or current density of a circuit; optical transduction which relies on the analyte's absorption or emission of light, either for direct visual observation or to generate an electrical signal; and mechanical transduction in which the analyte prompts a change in the shape (deflection) or motion (oscillation) of a mechanical component such as a cantilever or piezoelectric membrane, which in turn is transduced to an electrical signal. In some cases, of course, the physiological signal itself is electrical, in which case transduction is simply the reception and conditioning of the physiological electrical impulse.

2.1. Electrochemical transduction

Typical electrochemical systems are arranged in a three-electrode configuration in which the working electrode measures the potential established by the metal/electrolyte interface versus a reference electrode (*e.g.* a Ag/AgCl electrode) and a counter electrode completes the circuit. The electrochemical signal results from the diffusion of the targeted analyte from the bulk environment to the working electrode or to an analyte-sensitive material placed between the working and counter electrodes. A shift in potential at the working electrode (potentiometric), a change in conductance of the electrolyte between the working and counter electrode, an accumulation of charge (coulometric), or a rise or decrease in current (amperometric) indicates a change in concentration of the sensed molecule (Gencoglu and Minerick, 2014; Li et al., 2007). Electrical impedance spectroscopy is an additional, alternating current technique to sense changes in charge transfer resistance or capacitance on an electrode. As most of the integral components of electrochemical sensors are electrical circuit components, they are particularly well-suited to optimization using MEMS technology. Metal electrodes, insulating materials and catalysts can all be arranged in thin layers and patterned at the micron scale to create precisely ordered arrays of electrodes which are easily integrated with other circuit components.

2.1.1. Glucose sensors

The global market for continuous glucose monitoring systems was nearly $0.6 billion in 2015 and is expected to exceed $6.0 billion by 2022 (Allied Market Research, 2016). This growth is driven not only by increasing prevalence of diabetes (WHO, 2017) and improved access to health resources (French et al., 2016), but also by tremendous progress in glucose sensing technology. Transcutaneous glucose sensors the size of a needle now provide real-time blood glucose levels, allowing patients to monitor minute-to-minute fluctuations in their blood glucose throughout the day(US-FDA, 2016a,b). Their accuracy and reliability has permitted their use for automatic feedback in an insulin pump system; in late 2016 Medtronic's MiniMed 670G system became the first-ever truly closed-loop drug delivery system approved by the U.S. Food and Drug Administration (US-FDA, 2016a). The signal transduction for the 670G system, along with most other continuous glucose sensors is electrochemical. First, glucose is enzymatically oxidized at the electrode surface producing hydrogen peroxide as a product. Besides converting the glucose to a more chemically active chemical, enzymes provide the selectivity that helps ensure that only the target analyte influences the output signal. Immobilized glucose oxidase is the standard oxidizing enzyme on most glucose-sensing electrodes, though glucose-1-dehydrogenase and hexokinase have also been used (Yoo and Lee, 2010). Stoichiometric amounts of hydrogen peroxide are produced based on the local glucose concentration. Hydrogen peroxide is then oxidized, producing an electrical signal detected by one of the methods described earlier (*e.g.* amperometric, potentiometric, *etc.*). The immobilized enzyme and electrode are typically covered with a membrane to slow the transport of glucose to the electrode. This creates a constant, dominant transport resistance, dwarfing any variable physiological transport resistance to ensure that the rate of glucose reaching the electrode for oxidation is precisely proportional to the concentration of glucose in the blood. For oxygen-dependent enzyme systems, the membrane must allow a larger flux of oxygen, to ensure that it is always in excess so that glucose is always the limiting analyte being measured. And, it should prevent other oxidizable physiological species (*e.g.*, ascorbic acid) from reaching the electrode and influencing the reading. All of these functions are enhanced by increased membrane resistance, but that results in decreased hydrogen peroxide concentrations requiring increased sensitivity to hydrogen peroxide and lower peroxide detection limits. Alternatively, the electrode may catalytically reduce the remaining oxygen, comparing the depleted oxygen concentration around the immobilized glucose enzyme against the non-depleted oxygen concentration measured by a separate reference sensor (Gough et al., 2010; Lucisano et al., 2017). Fully implantable sensors using this approach have functioned in pigs for over a year (Gough et al., 2010) and were just demonstrated in humans for six months (Lucisano et al., 2017). This follows the footsteps of six-month trials of fully implantable peroxide-based glucose sensors dating back well over a decade (Gilligan et al., 2004).

These implantable systems in particular underscore the importance of MEMS technology to electrochemical biosensing, where the electrodes are integrated with the circuitry needed to drive the system and wirelessly transmit the output signal (McKean and Gough, 1988), reducing the footprint and power consumption of the system significantly. Moreover, MEMS technology has helped push the detection limit of hydrogen peroxide using electrochemical sensors down to submicromolar concentrations. The simplest example of an electrode for hydrogen peroxide oxidation is a strip of bare platinum (Kim et al., 1999; Zhu et al., 1994). Dividing this strip into an array of Pt working electrodes has been shown to increase hydrogen peroxide detection through increased total charge accumulation (Sassa et al., 2010). Spacing, size, and number of Pt strips have been optimized to increase the total charge in this coulometric detection technique with 40, 10 μm-wide electrodes spaced 10 μm apart. The limit of H_2O_2 detection using this array reached 410 nM H_2O_2. Other metal catalysts that have been micropatterned to decompose hydrogen peroxide include iridium, palladium, gold, silver, and manganese dioxide (Chen and Chatterjee, 2013). One glucose sensor currently in clinical trials uses an array of eight electrodes made from carbon paste, glucose oxidase, and

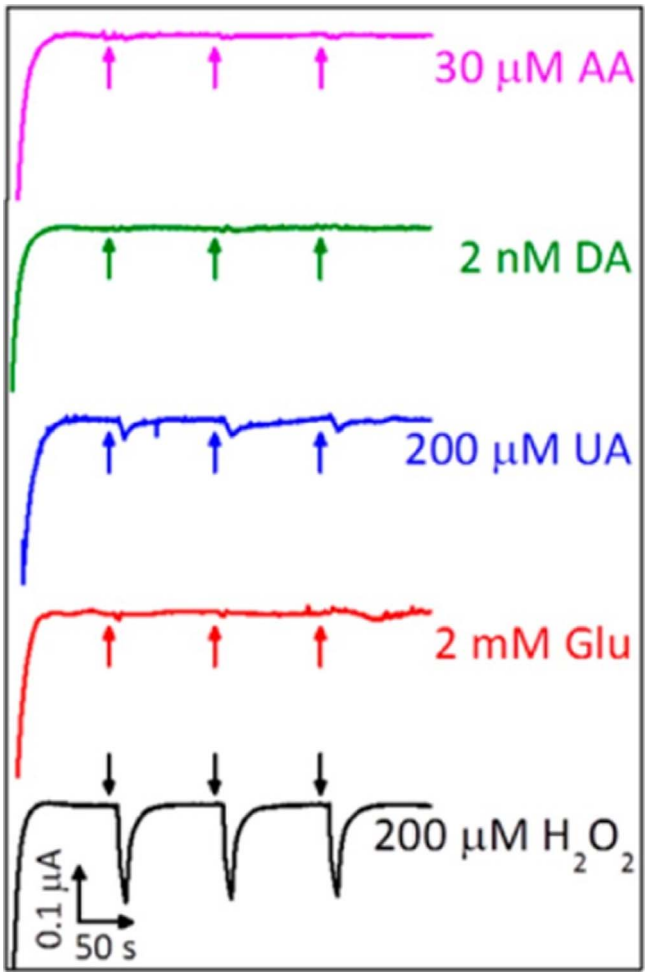

Fig. 1. Amperometric detection of hydrogen peroxide oxidation on WS_2 electrode for glucose detection in the presence of ascorbic acid (AA), dopamine (DA), uric acid (UA), and glucose (Glu). Arrows indicate time points of analyte injection. Reproduced with permission from (Toh et al., 2017).

manganese dioxide microfabricated within a $1 \times 6\,mm^2$ area (Schmelzeisen-Redeker et al., 2013; Zschornack et al., 2013). This manganese dioxide electrode exhibited a 0.35 V *vs.* Ag/AgCl oxidation potential for hydrogen peroxide which may prevent oxidation interference from other analytes in the body.

In pursuit of eliminating interfering oxidation currents, researchers have turned to novel materials apart from noble metals and their oxides. Group 6 transition metal dichalcogenides (TMD) are a class of inexpensive metal electrodes that include MoS_2, $MoSe_2$, WS_2, WSe_2 and have been used to demonstrate hydrogen peroxide detection (Toh et al., 2017). They can be deposited in thin films *via* magnetron sputtering which makes them ideal for MEMS fabrication (Chia et al., 2015; Koçak et al., 2016). In particular, WS_2 demonstrated the highest current densities with a detection limit as low as 2.0 nM H_2O_2. Interfering analytes demonstrated low to negligible oxidation currents on this WS_2 electrode in the presence of hydrogen peroxide oxidation at 0.5 V *vs.* Ag/AgCl as shown in Fig. 1. Other types of nonenzymatic detection mechanisms for hydrogen peroxide that can be incorporated into MEMS devices include the use of carbon based materials, nanostructured metals, and conductive polymers (Barsan et al., 2015; Chen and Chatterjee, 2013).

Just as enzymes convert glucose to a more accessible chemical signal such as hydrogen peroxide, enzymes will also convert hydrogen peroxide to the desired electrical signal. Using horseradish peroxidase covalently bound to glutathione-coated gold nanoparticles decorating gold wire, 5 nM H_2O_2 detection was achieved (Chikkaveeraiah et al., 2009). While no interfering biological analytes were present in this MEMS-enhanced detection limit trial (as opposed to the WS_2 case mentioned previously), the selectivity of these enzymes (Ferri et al., 2011; Kuo et al., 2015) should preclude any false signal from other chemical species.

2.1.2. pH sensors

Besides glucose, pH is an important physiological chemical signal which is typically detected electrochemically. With different ideal values in different parts of the body often inaccessible by wires, these sensors typically must be integrated with all of the driving, conditioning, and telemetry circuitry needed to wirelessly transmit a signal, making MEMS technology critical to their feasibility. An IrO_x electrode has been fabricated on a flexible polyimide circuit for pH detection over a range 2.0–11.0 with response times as fast as 0.9 s (Cao et al., 2012; Huang et al., 2011). This sensor was fabricated next to an impedance sensor to produce a dual sensing, implantable device for monitoring esophageal reflux events. The impedance component monitored when a reflux event occurred (wetting the sensor changes the ion concentration between gold electrodes corresponding to changes in impedance) while the pH sensor detected shifts in acidity as a function of the potential between the IrO_x and Ag/AgCl reference electrodes. By comparison, a current commercially available sensor—the Bravo pH monitoring device by Medtronic—is fabricated from antimony but does not include the impedance sensing component and failed to detect reflux events in the esophagus when back-to-back events are of similar or neutral pH (Kwiatek and Pandolfino, 2007).

2.1.3. Gas sensors

Physiological gases represent a third class of analytes whose detection would be useful in a closed-loop drug delivery mechanism, as demonstrated above for measuring the enzymatic oxidation of glucose by monitoring oxygen concentration. Efforts to administer oxygen as a drug (Pilcher and Beasley, 2015) similarly require rapid, accurate oxygen saturation measurements. Oxygen concentration can be measured *via* its reduction on metal catalysts; typically platinum is used as the sensing electrode (Kumosa et al., 2014). Improvement in current densities using an amperometric technique has been observed when a palladium catalyst is deposited on nanoporous aluminum oxide templates with either 100 nm or 200 nm pore sizes (Do et al., 2016). Conversely, organic gases can be measured by their oxidation on metal catalysts (Griveau and Bedioui, 2013). To prevent fouling and increase sensor lifetime, nitric oxide (NO) generation next to an oxygen sensor was shown to increase the reliability of the oxygen partial pressure measurement when compared to measurements without NO generation (Ren et al., 2015). The ability to inexpensively mass produce such cells with MEMS circuitry likely facilitated the popularity of personal blood alcohol sensors and carbon monoxide detectors.

2.1.4. Other electrochemical sensors

Using e-beam nanolithography, Esfandyarpour et al. have demonstrated the fabrication of multilayered nanoneedles with 10 nm diameter tips that detect absorbed analytes through shifts in impedence (Esfandyarpour et al., 2013). The aim of developing such small electrode tips is to enable them, when functionalized with a selective antibody, to detect a single molecule of the corresponding antigen. Fabricating these tips in an array would enable simultaneous detection of multiple analytes by the same sensor. Detecting low concentrations of antigens has already been realized using miniaturized complementary metal oxide semiconductor (CMOS) interdigitated microelectrodes. These microelectrodes are among several methods enabled by microfabrication that can detect DNA concentrations in the fM range using impedimetric techniques, largely based on capacitive changes between microfabricated plates (Ferrier et al., 2015; Lai et al., 2012).

In the same vein, electrode surfaces are also commonly integrated into field-effect transistors (FETs) in which a current source and drain

are separated by a gate whose resistance changes based on interactions between the gates' material and analytes in the surrounding environment. The selectivity of the membrane gate for a specific ion or molecule ensures that only one analyte will be detected by the FET. Semipermeable membranes have been used in ion selective FETs for detecting K^+, Na^+, or Ca^{2+}, or membranes functionalized with enzymes to sequence DNA (Kataoka-Hamai and Miyahara, 2011; Lee et al., 2009).

2.2. Optical transduction

From a lab-bench perspective, optical methods for measuring biomolecules such as absorption, fluorescence, interferometry, and surface plasmon resonance (SPR) are ideal quantification techniques since their components (excitation lasers, fiber optic cables, lenses, mirrors, detectors) can be precisely aligned to detect low analyte concentrations with higher signal-to-noise ratios (Myers and Lee, 2008; Rodríguez-Ruiz et al., 2016). However, shrinking these components to the size needed for an implantable biosensor does not result in the same benefits seen with the electrochemical sensors (faster response time, decreased detection limits). This is because optical detection often relies on attenuation of a light source as it interacts with the analyte. This attenuation is more easily detected with increased sample volume or path length as governed by the Beer-Lambert law. Thus, reducing the sample volume when creating a microfabricated device actually hinders the quantification method. Still, researchers have circumvented these challenges while attempting to implement the benefits of an optical detection method in a biosensor. The applications of MEMS technology towards reducing the size of the various optical components is discussed next followed by applications to optical glucose and blood pressure sensing.

2.2.1. Microfabricated optical components

The light sources and detectors needed for sensing applications have been miniaturized using microfabrication for a decade to create submillimeter light emitting diodes (LEDs) and photodiode arrays (Balslev et al., 2006; Chang et al., 2011; Irawan et al., 2007). These components are typically assembled in external microfluidic devices that would be quite large (a few square centimeters) for an implantable biosensor in order to probe a larger volume of the liquid of interest, though efforts to reduce the required sample size, and hence device size, continue. Shrinking the area between the light emitter and detector where the sensing occurs requires maximizing light interactions with the analyte without increasing the sample volume. One approach uses microfabricated lenses and mirrors in poly(dimethylsiloxane) (PDMS) to increase the path length while reducing areas of 'dead space' in the sample volume that do not contribute to enhancing the signal (Llobera et al., 2007). These air mirrors are curved PDMS elements separated from the sample chamber by a thin gap of air. Taking advantage of the different refractive indices of air and PDMS, light is reflected back into the sample volume and focused to a smaller volume than the original light input as shown in Fig. 2. Zigzagging the reflected light between multiple mirrors down the length of a flow channel or sample volume increases the optical path length without increasing the fluidic path length. Eliminating the dead space not occupied by the optical path, the sample volume was reduced by a factor of 2.3 while retaining the same detection limit (approximately 110 nM for fluorescein, a common fluorescent tracer molecule). Organizing three mirrors into a ring structure, the optical path was increased by a factor of 1.7, resulting in a 50% decrease in the fluidic path length from the two-mirror structure and a lower 41 nM detection limit for fluorescein.

Optical waveguides act to collect and direct light to different areas of a device; their background and application to integrated optical sensors has been reviewed (Lambeck, 2006). If the aim of an optical-MEMS sensor is to increase the amount of light-analyte interactions without increasing the sample volume, then photonic nanofences (PNF)—a type of waveguide—may satisfy this aim as was recently demonstrated by Cadarso et al. (Cadarso et al., 2016). They optimized the intensity of an evanescent field (EF) by reducing the size of the rectangular cross-section of the fence in only one dimension below the wavelength of the input light; *e.g.* a 635 nm laser projected on a 250 nm-wide PNF. Direct laser writing was used to create the 6–10 μm tall PNF, ensuring homogenous, 250 nm thickness down the length of millimeters-long fence as shown in Fig. 3. By spacing two, 250 nm-wide nanofences 5 μm apart, 90% of the light coupled to the PNFs was emitted as an EF as shown in Fig. 3. The EF interacts with the surrounding medium, increasing the width of the sensing area eight times over the wavelength of the incident light. The utility of this feat was demonstrated in an absorbance sensor by coating the PNFs with an ion-sensitive ionophore immobilized in a poly(vinyl chloride) membrane as a sensor for lead. A whole host of ionophores/fluorescent tags could be immobilized over the PNFs for biosensing with the light energy provided by the EF at the PNF/membrane boundary.

2.2.2. Glucose sensors

Despite the challenges with miniaturizing optical sensors, they have made their way into the glucose sensing market. In fact, a fluorescent-based glucose sensor made by Senseonics recently demonstrated 90 days of continuous use in an *in vivo* trial in which the sensor was implanted into the arms of 24 patients (Dehennis et al., 2015). This device houses an LED excitation source, filtered photodiodes, and a wirelessly powered transmitter all within a 3.3 mm-diameter, 15 mm-long cylinder, shown in Fig. 4 (Colvin and Jiang, 2013; Mortellaro and DeHennis, 2014). The sensor does not rely on a glucose-sensitive enzyme for the detection mechanism, which the inventors claim will degrade over time and contribute to the relatively short (5–7 days) lifetime of the electrochemical glucose sensors discussed earlier. Instead, glucose diffuses through a semipermeable membrane and interacts with a fluorescent tag copolymerized with poly(2-hydroxyethyl methacrylate) (pHEMA) to create a glucose-sensitive membrane. The authors also demonstrated improved sensor lifetime when the protective membrane was coated with 10 nm of platinum that serves to oxidize any hydrogen peroxide generated during the wound healing process that would otherwise destroy the fluorescing molecule in the sensor (Colvin and Jiang, 2013). In clinical trials, the implanted sensor's glucose measurement was compared with blood glucose levels obtained intravenously. The Mean Absolute Relative Difference (MARD) between the sensor and gold-standard IV measurements was 11.4 ± 2.7% over the entire 90 day clinical trial (Dehennis et al., 2015).

Enzymatic-based glucose sensors have also been used to detect glucose optically, though indirectly, by measurement of the oxygen concentration (Su et al., 2017). As mentioned earlier, the difference in oxygen concentration between a reference cell and one enzymatically consuming stoichiometric amounts of oxygen and glucose will indicate the glucose concentration. In this case the oxygen concentration was measured optically by its ability to quench fluorescence in each cell. Using MEMS technology, this approach may be miniaturized to an implantable scale.

2.2.3. Blood pressure sensors

Blood pressure monitoring has been proposed to facilitate treatment of hypertension in implementing a closed-loop drug delivery system. One example of an implanted blood pressure MEMS device uses both optical and electrical components (Theodor et al., 2013). The optical transduction mechanism uses an LED and adjacent photodiode to detect changes in absorption due to volume changes in pulsating blood vessels in the surrounding tissue. This signal is measured at the same time as an electrocardiogram (ECG) from gold electrodes on the same device; both are transmitted wirelessly. The sensor was tested *in vivo* using a sheep model by implantation next to the carotid artery. Deviations of the sensor's measured blood pressure versus an intra-arterial reference measurement was 5.5 mmHg. Microfabricated optical biosensors of this

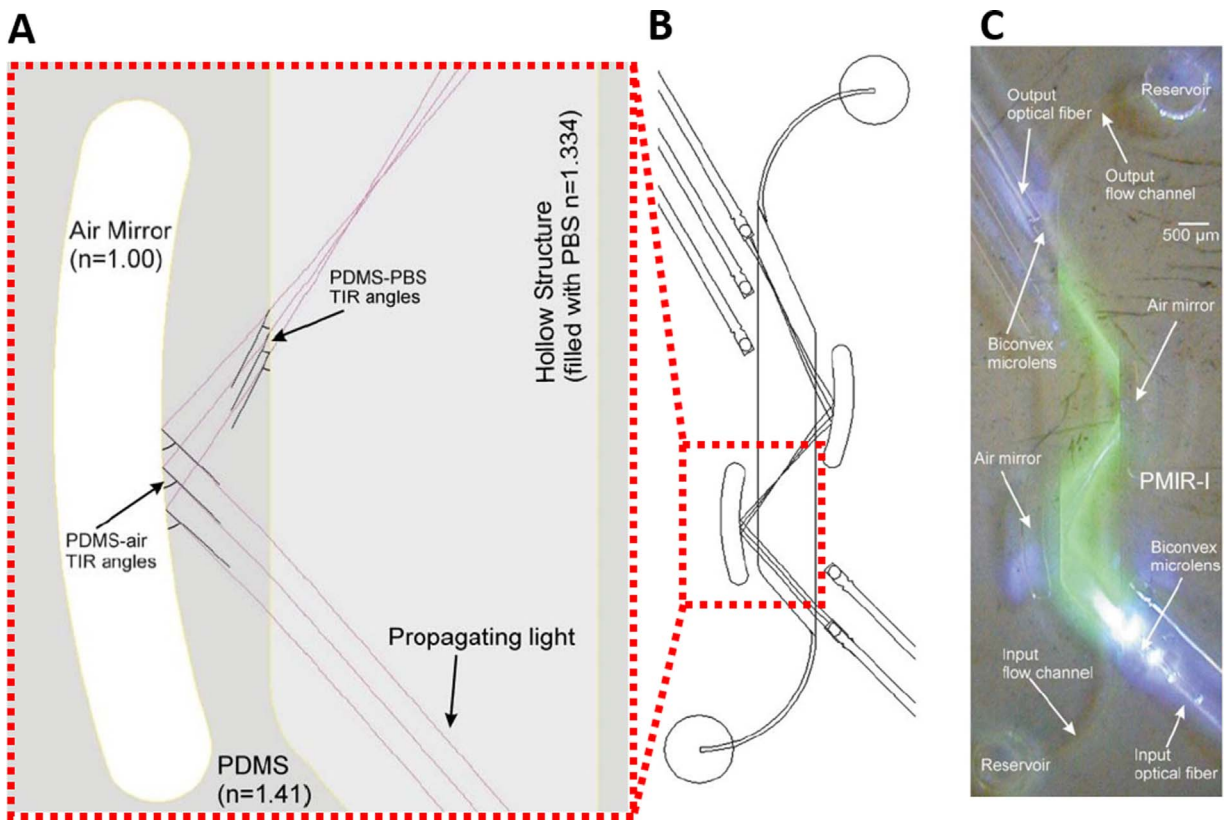

Fig. 2. Optical air mirrors for fluorescence detection. A) and B) Different refractive indices of air (n = 1.00) and PDMS (n = 1.41) used to create mirror to focus light down longer optical path length. C) Optical micrograph of B). Reproduced with permission from (Llobera et al., 2007).

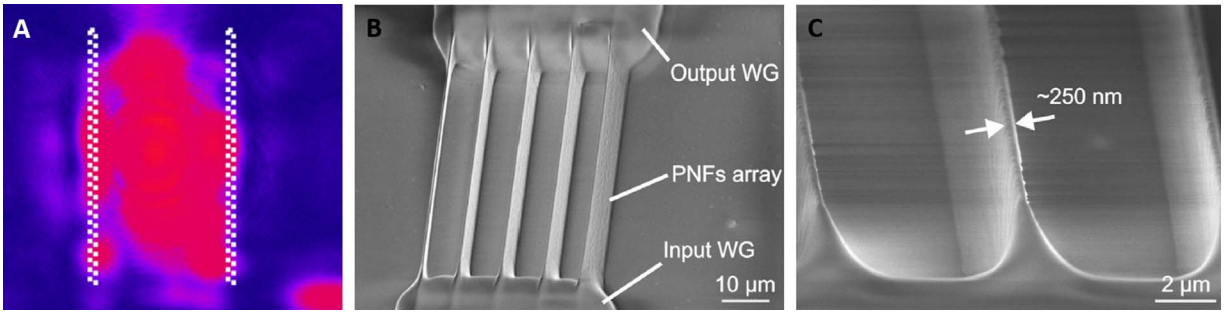

Fig. 3. Photonic nanofences (PNFs) for optical sensing. A) Near field light distributions between two nanofences (dotted lines) separated 5 µm apart. B) and C) SEM images of nanofences. Reproduced with permission from (Cadarso et al., 2016).

type may be most practical since it does not require long optical path lengths or interactions with a diffusing analyte for increased absorption.

2.3. Mechanical transduction

This section addresses both transduction from a chemical signal to a mechanical signal, as well as transduction from a mechanical signal to an electrical one. The former typically involves the integration of both hard and soft materials, whose interaction with each other is influenced by the chemical analyte; for example, a soft hydrogel constrained in a rigid enclosure. The presence of a particular analyte may prompt the constrained hydrogel to swell, increasing the pressure in the enclosure. Because this type of transduction requires the analyte to interact with a bulk material, rather than a surface, miniaturization through MEMS technology is critical to performance; the transport time of the analyte into (and out of) the bulk material scales with the square of the material's thickness. As a result, significant effort has gone into the integration of hard and soft materials in MEMS fabrication (Siegel et al., 2010; Ziaie et al., 2004). Transduction of this mechanical signal to an electrical one may be done directly, for instance by allowing the increased pressure of the enclosure to deflect a capacitor plate, or indirectly by optically transducing a position change to an electrical signal. These mechanical-to-electrical transduction mechanisms are integrated to the MEMS-based chemical-to-mechanical ones, though even stand-alone mechanical-to-electrical transductions for biosensors are typically performed by MEMS devices because of their tiny footprint, low power consumption, and high reproducibility.

2.3.1. Mechanical-to-electrical Transduction: pressure sensors

MEMS-based pressure sensors have been studied to address a variety of medical maladies including sleep apnea (air pressure), dehydration (osmotic pressure), heart failure (blood pressure), glaucoma (intraocular pressure), and hydrocephalus (intracranial pressure) (Apigo et al., 2016; Chen et al., 2010; Chow et al., 2010; Costanzo et al., 2016; Fernandes et al., 2016; Jin and Sanchez-Sinencio, 2015; Kawoos et al.,

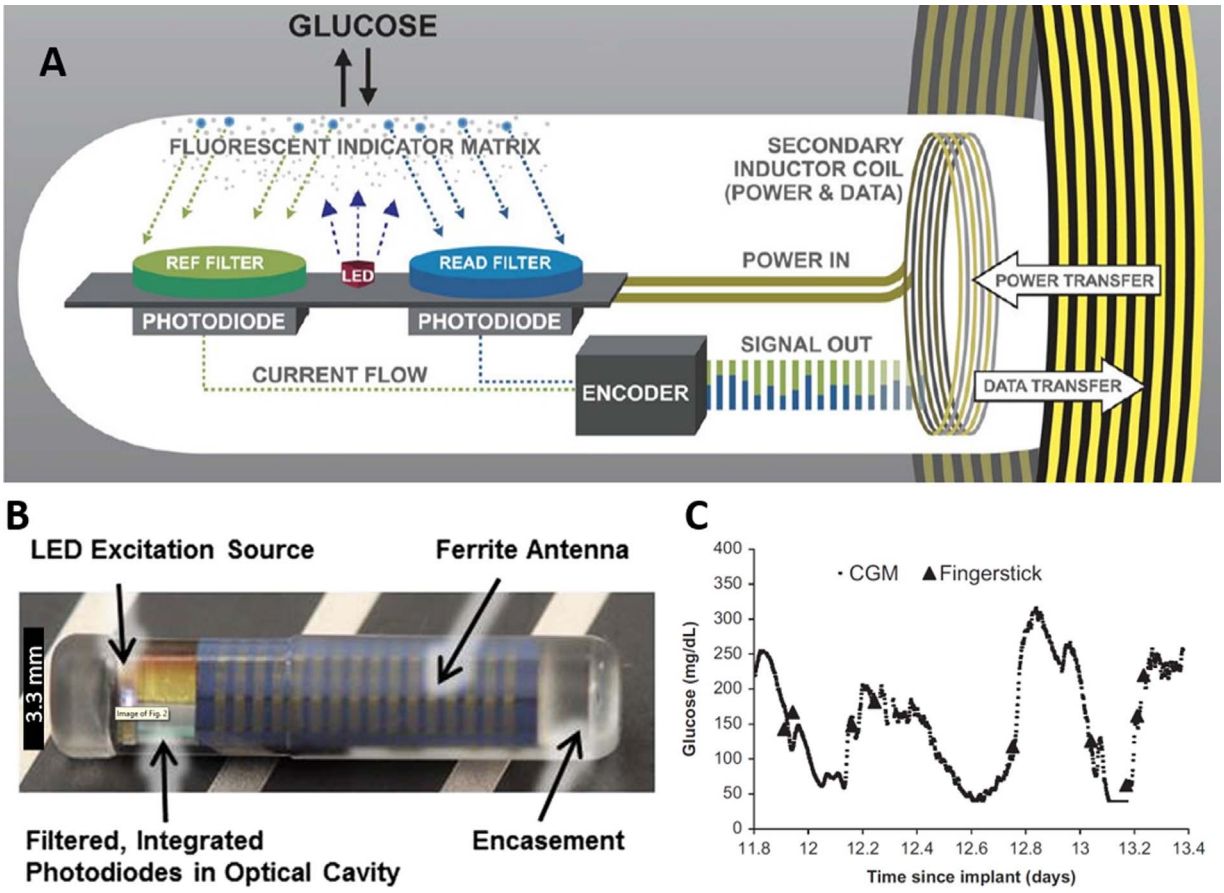

Fig. 4. Optical sensor for continuous glucose monitoring (CGM). A) Schematic of sensor B)optical micrograph of sensor. C) Glucose concentration *vs.* time from CGM implanted in patient compared to traditional finger-stick measurement. Reproduced with permission from Colvin and Jiang (2013) and Mortellaro and DeHennis (2014).

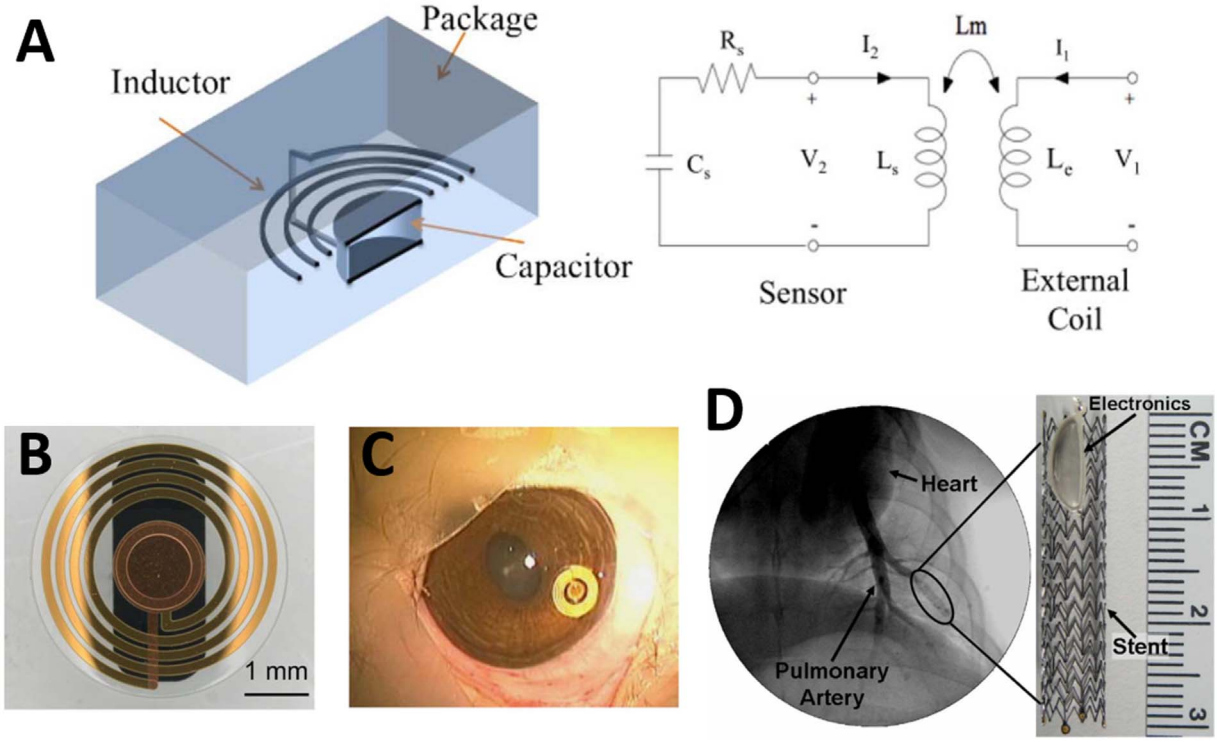

Fig. 5. Wireless capacitive pressure sensors. A) Schematic cross section of a diaphragm cell capacitor (left) and an equivalent circuit (right) of a passive resonance frequency sensor. B) Optical micrograph of flexible, ocular pressure sensor C) implanted on the iris of a rabbit eye. D) Pressure sensor mounted on a stent and implanted in a pig pulmonary artery. Reproduced with permission from Luo et al. (2014), Chen et al. (2010), and Chow et al. (2010).

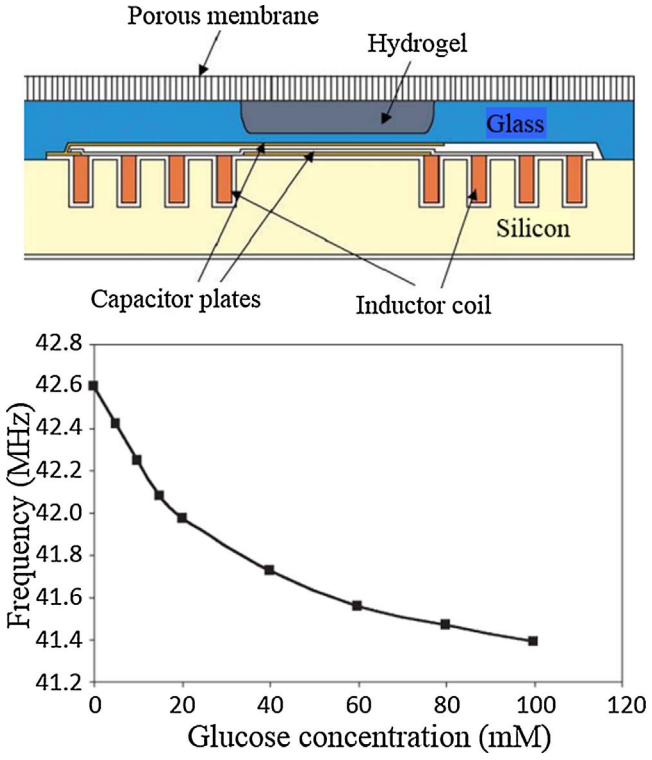

Fig. 6. Hydrogel-Based MEMS transponder for wireless glucose measurement. Top) Schematic of transponder. Bottom) Resonance frequency of transponder *vs.* external glucose concentration. Reproduced with permission from Lei et al. (2006).

2008). These capacitive pressure sensors are microfabricated in order to overlay all the sensing and transmitting components onto the same space, occupying only a few square millimeters. The sensor involves a passive, wireless impedance measurement based on deflection of a diaphragm holding a capacitor plate connected to a radio-frequency (RF) induction coil as shown in Fig. 5 (Castanheiro et al., 2006). This capacitor-inductor circuit has a specific resonance frequency which can be wirelessly interrogated by a transmitter external to the body. This resonance frequency shifts with the thickness of the gap between the capacitor plates. Increased pressure reversibly deflects the diaphragm, narrowing the gap between the capacitor plates and shifting the resonance frequency. Capacitive pressure sensors have been fabricated as small as 4 mm diameter on flexible substrates, implanted directly into the eye, and anchored on the iris as was shown in an *in vivo* rabbit model for monitoring intraocular pressure for the purposes of treating glaucoma (Chen et al., 2010).

In one study, similar components were microfabricated on biodegradable materials using zinc/iron alloys and hydrolytically degrading poly-L-lactide/polycaprolactone materials (Luo et al., 2014). The metal components were first microfabricated on a rigid, silicon wafer then transferred to the degrading polymer sheets. The device's resonant frequency was monitored over the course of its degradation in a saline solution with normal sensing lasting 107 days. The time for channels to percolate across the degrading polymer to the capacitor gap may determine the sensor lifetime; this time may be modeled based on the polymer's thickness, permeability, and hydrolysis rate constant (Coffel et al., 2016).

An FDA-approved, capacitive pressure sensor has been used for monitoring pressure in the pulmonary artery to aid treating symptoms associated with heart failure (HF). All components of the sensor are microfabricated to fit within a 15 mm by 3 mm area. The sensor is hermetically sealed in a fused silica capsule and provides real-time pressure monitoring that is transmitted wirelessly to a display screen (Castro et al., 2007). This device—St. Jude's CardioMEMS™ HF system—was attributed to reduced heart-failure-related hospitalization by 37% compared to patients without the monitoring system (Abraham et al., 2011). Calls for treating congestive HF symptoms based on information provided by an implanted pressure monitoring system have been proposed since the 1990s (Steimle et al., 1997; Stevenson, 1999). Recently, a 2016 study was the first to link the decrease in HF-related hospitalizations reported in the 2010 CardioMEMS™ study to more frequent active changes in the patients' medication (*i.e.* the drug dosing schedule) as a result of hemodynamic information provided by the device (Costanzo et al., 2016). One can easily envision taking this a step further to implement a closed-loop system that would automatically adjust drug delivery rates of vasodilators and diuretics (both drugs used to treat HF symptoms) based on hemodynamic measurements from the implanted pressure sensor—similar to that for controlling blood glucose levels in diabetes patients.

2.3.2. Chemical-to-mechanical Transduction: hydrogels

Hydrogels are crosslinked polymer networks which absorb a substantial amount of water, often several times their dry weight. This equilibrium swelling can be tuned by a variety of stimuli including temperature (Hirokawa and Tanaka, 1984; Klouda, 2015), pH (Hirotsu et al., 1987; Siegel and Firestone, 1988), ionic strength (Tanaka et al., 1980), and light (Jochum and Theato, 2013; Sumaru et al., 2004). Moreover, this sensitivity can be programmed by grafting specific chemical groups onto the polymer, instilling sensitivity to specific chemicals such as glucose (Kataoka et al., 1998; Wang et al., 2017a), antigens (Miyata et al., 1999), or nucleic acids (Tang and Xiao, 2009; Wang et al., 2017b). Enzymes can also be entrapped in these networks, providing another route to chemical-specific signal transduction (Zhao et al., 2017). As a result, hydrogels provide a powerfully versatile platform for transducing chemical signals to mechanical ones (Peppas and Van Blarcom, 2016). One of the major drawbacks to hydrogel sensing, however, is slow response time. The equilibrium swelling state is not reached until the chemical analyte has diffused throughout the entire gel and water has subsequently entered or exited; these processes may take several hours for millimeter-scale monoliths of homogenous hydrogel. The response time decreases with the square of the hydrogel thickness (Li and Tanaka, 1990), however, making miniaturization to the MEMS scale critically important. Moreover, by mechanically constraining the hydrogel to its shrunken volume and measuring the pressure required for this constraint, the hydrogel thickness can be kept small and the need for water transport eliminated (Deng et al., 2018).

There are a variety of mechanisms for subsequently transducing hydrogel swelling to a transmittable signal. One attractive approach is incorporation with the capacitive pressure sensors discussed above. Fig. 6 is a schematic of such a sensor with a 200 μm-thick film of poly (acrylamide-co-methacrylamidophenylboronic acid) (80/20 by mol) hydrogel atop a flexible capacitor plate attached to an embedded induction coil, above a plot of the device's resonance frequency as a function of surrounding glucose concentration (Lei et al., 2006). Mounted on a piezoelectric element, hydrogels will alter the element's resonant frequency as it swells (Kanekiyo et al., 2000). Similarly, hydrogels have been mounted on magnetoelastic elements to change their resonant frequency in response to pH (Ruan et al., 2003); incorporation of a pH-lowering enzyme allowed detection of 10^{-7} M concentrations of organophosphorus pesticides (Zourob et al., 2007). Hydrogels have also been mounted above (Hilt et al., 2003) or below (Lei et al., 2007) microscale cantilevers, deflecting them as the hydrogel swells. Transducing that deflection to a transmittable signal requires a second process, however, such as optically querying the microcantilever position by reflecting a laser beam off of it onto a photoreceptor array.

Hydrogel swelling can be optically queried directly, however, by mounting a film of the hydrogel on an optical fiber and observing the phase change of the reflected light as the size of the hydrogel element changes (Gawel et al., 2010). Alternatively, the hydrogel can be used to form a colloidal crystal whose diffraction shifts with swelling (Kabilan

et al., 2005; Muscatello et al., 2009). Similarly, dispersing magnetic nanoparticles in a hydrogel, the magnetic permeability of the gel changes as it swells or shrinks, which alters the resonance frequency of an adjacent MEMS circuit (Song et al., 2014). By incorporating a conducting copolymer, hydrogels have also been used to transduce chemical signals directly to electric ones, changing their conductivity in response to analyte concentration(Bayer and Peppas, 2008; Brahim et al., 2003).

The mechanical response of hydrogels to chemical concentrations can be taken a step further, however. Rather than transducing the chemical signal to (eventually) an electrical signal reported to the patient, who must then intervene to alter subsequent drug dosing, the hydrogel's swelling response may be used to directly actuate delivery of a drug, providing completely automated, closed-loop drug delivery. Many variations of positive feedback delivery valves have been demonstrated from immobilizing stimuli-sensitive hydrogel nanoparticles in a polymer membrane(Zhang et al., 2004) to mounting the hydrogel in micron-scale orifices in microfabricated silicon wafers(Baldi et al., 2006) to MEMS-scale conventional plunger valves(Eddington and Beebe, 2004; Siegel et al., 2010). In each case the valve relies on hydrogel swelling to close the valve and block release. This is opposite to the polarity typically required for closed loop drug delivery, however. Releasing a drug by swelling in response to another chemical (for instance, using a glucose-swelling hydrogel to open insulin release, rather than close it), requires the opposite polarity which has proven more difficult to achieve, though hydrogels which shrink in response to glucose or fructose have been demonstrated(Nguyen et al., 2018). The long term stability of the hydrogel must also be considered for any closed-loop application.

2.3.3. Chemical-to-mechanical Transduction: fluids

Fluids may also be used for chemical to mechanical transduction. Affinity viscometry in particular has attracted attention for glucose sensing(Birkholz et al., 2013; Birkholz et al., 2016). In this technique, the vibrational frequency of a microfabricated cantilever is measured in a fluid accessible to physiological glucose. The glucose concentration affects the medium's viscosity through interactions with dextran and concanavalin A; the latter is a protein with specific binding sites for glucose, conferring selectivity. The change in frequency due to damping by the fluid's variable viscous resistance is continuously transmitted and compared with a glucose-free reference. The entire sensor (360 μm by 1.3 mm) is shown in Fig. 7, which is then assembled with other telemetry components, a power supply, and a semipermeable membrane, all contained within a titanium housing.

2.4. Other transductions

Some physiological signals are already electrical, and only require retransmission, such as with neural recording or cardiac monitoring. The former, in particular, requires high spatial precision, often in a multichannel array, with as small of a footprint as possible, making MEMS technology ideal. Transduction of temperature to a transmittable signal is straightforward and easily implemented in MEMS devices, typically by measuring the change in resistance of a conducting element (thermistor) or the change in potential between adjacent, dissimilar metals (thermocouple). Temperature also shifts the optical absorption of semiconductors such as gallium arsenide, which are then used in optical sensors.

Besides being used to drive dosing decisions in drug delivery, biosensors may also be used to monitor diet(Prioleau et al., 2017) and dosing compliance(Hafezi et al., 2015). MEMS technology has enabled the mass manufacture of uniquely labelled wireless emission circuits, complete with battery, in a package less than 0.5 mm^3, small enough to place within most solid drug formulations. When immersed in a conducting liquid such as digestive fluids, the battery plates are electrically connected, prompting wireless emission at the circuit's unique frequency. An external receiver then receives the signal and records the patient's pharmaceutical compliance (Hafezi et al., 2015). These sensors have recently received US FDA approval as a component of aripripazole tablets for schizophrenia and other mental health diseases (US-FDA, 2017).

3. Challenges

MEMS-based biosensors face most of the same challenges as conventionally manufactured biosensors, most notably the foreign body response, though their materials limitations, their small size, and their propensity for integration with control, telemetry, and dosing elements alter these challenges.

3.1. Safety

Conventional MEMS materials (silicon, SiO, SiN, SU-8, various metals) have been tested extensively *in vivo* (Ferrara et al., 2003; Voskerician et al., 2003)and have been evaluated according to ISO 10993 standards(Kotzar et al., 2002) to demonstrate that they are as safe as other common materials for medical use. Moreover, the small size of MEMS devices decreases their power needs and their physical footprint, ostensibly reducing their potential electrical or mechanical risks. There is as yet no indication that MEMS sensors have a different infection risk than other devices, and their low power consumption and propensity for integration with wireless telemetry reduces the need for transcutaneous wires which would serve as an infection vector.

An emerging safety concern for wirelessly-communicating biosensors, however, is eavesdropping and hacking of the communications signal. Besides the invasion of privacy implicit in eavesdropping on the sensor transmission, either as it exits the body or is retransmitted further afield, an eavesdropper may also then mimic the signal, transmitting false information. If the mimicked sensor is used to determine subsequent drug dosing, the consequences of malicious interference could be tragic. Security demonstrations hacking internet-connected drug infusion pumps have already prompted the US FDA to issue warnings recommending that the product's use be discontinued (US-FDA, 2015). Another manufacturer has noted that its insulin pump system is vulnerable to local hacking through its remote control interface (Finkle, 2016). While these attacks targeted the drug delivery component directly by mimicking the command signal, similar effects could in principle be achieved by hijacking the sensor signal to deliver false readings which would prompt incorrect dosing commands, even in an open-loop system with human oversight. One approach to minimizing these security vulnerabilities is to keep the entire dosing/sensing loop on closed circuits within the body with routine outbound broadcasting of sensor values and delivery activity, but with infrequent inbound broadcasting requiring more significant user intervention. Using MEMS technology, the biosensor, control module, and drug delivery vehicle can much more easily be integrated together as a closed-loop drug delivery device.

3.2. Power

Another significant challenge for implantable biosensors in particular is powering them. Batteries occupy a significant amount of space and often contain hazardous components. One of the advantages of MEMS devices over conventionally fabricated devices is that their power consumption often scales with their size, greatly reducing the battery size required for a given device lifetime. Moreover, many MEMS sensors, particularly capacitive pressure sensors containing an induction coil, operate passively, relying on a powered external device to interrogate them by transmitting an electromagnetic signal which the sensor absorbs and re-emits differently depending on its state (Lei et al., 2006, 2009). Along a similar vein, circuitry to convert that externally supplied electromagnetic energy into power for the implanted device

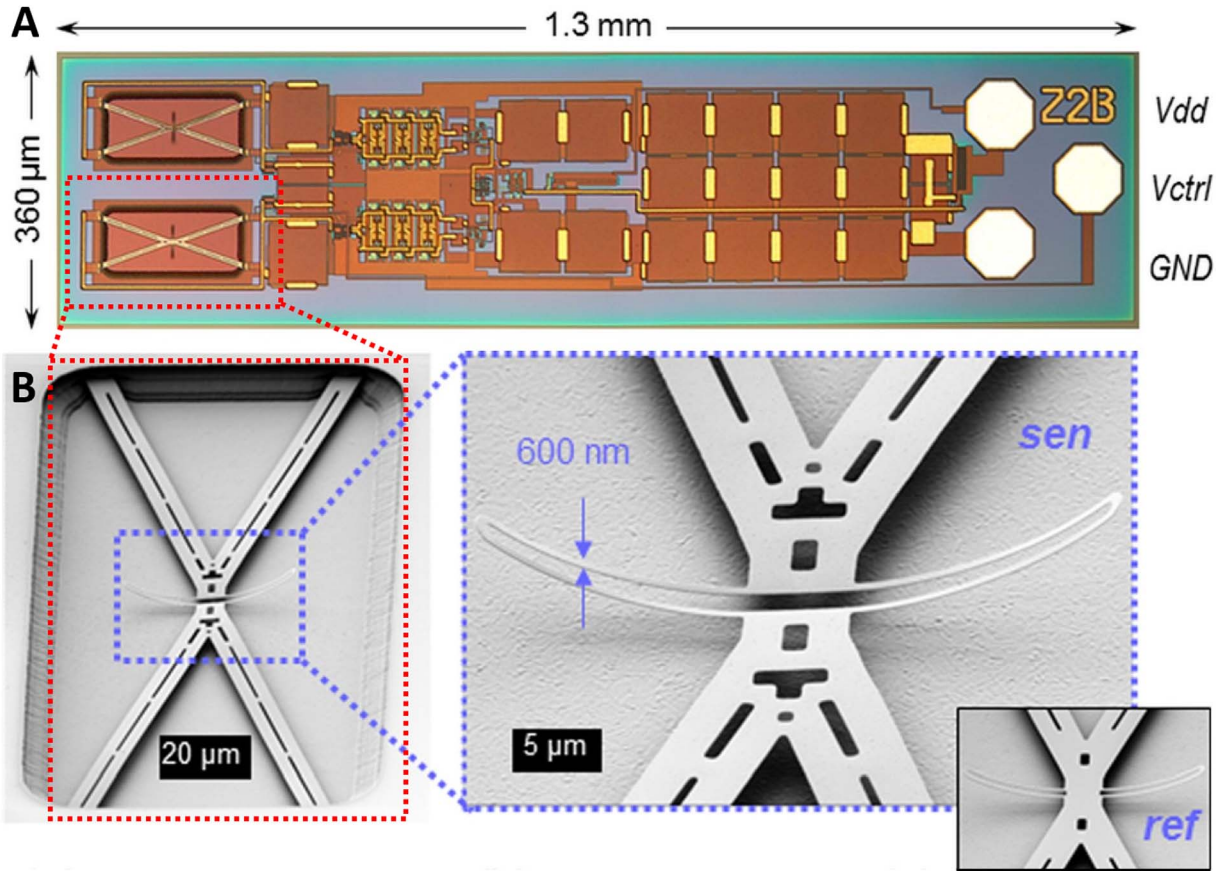

Fig. 7. Affinity viscometer for glucose sensing. A) Optical micrograph of entire sensor including reservoir for deflecting beam, capacitor, and contact pads. B) SEM images of deflection beam in empty reservoir. Reproduced with permission from Birkholz et al. (2013).

can be readily integrated into MEMS devices (Weir et al., 2009), and significant effort has been put to developing CMOS circuits for inductively coupled wireless power transfer (Sauer et al., 2005). Other modes of wireless power transfer, such as ultrasonic transmission (Ozeri and Shmilovitz, 2010), have also been investigated but are less prevalent. Harvesting power from the body has also attracted significant attention (Cadei et al., 2014), ranging from simple electromechanical devices to fuel cell devices which not only sense glucose but use it to power themselves as well (Slaughter and Kulkarni, 2017).

3.3. Corrosion

While traditional MEMS materials may be safe for the human body, the human body is not necessarily safe for traditional MEMS materials, particularly over the lifespan expected of an implanted device. The most common MEMS material, silicon, will dissolve in the body over a length scale of days to months, depending on the porosity and thickness of the material (Hämmerle et al., 2002; Wang et al., 2007). This property has actually been used as a feature in the development of drug delivery vehicles, where drug is loaded and released from sacrificial porous silicon chips. Passivating the surface with more robust materials like silicon oxide or silicon nitride is a routine MEMS procedure, as those materials also electrically insulate the underlying semiconductor. However, though they are more robust than silicon, they still dissolve in the body (3.5 and 0.33 nm/day, respectively (Maloney et al., 2005)) and their common deposition techniques are prone to producing pinholes (Hämmerle et al., 2002; Schmitt et al., 1999) which may be too small to matter in air-based insulating conditions, but which prove fatal to the underlying silicon when immersed in physiological liquids for an extended period. The silicon itself may be oxidized to form a much denser silicon oxide protective layer, but the hours at > 900 °C required for this oxidation are often infeasible for biosensor construction, particularly sensors with enzymes or multi-functional polymer transducing agents. This has prompted significant study into less common, but more inert, materials such as sapphire and diamond. Sapphire is already an attractive electrical insulator for applications requiring high thermal conductivity, high chemical stability, or high hardness, and has been incorporated into a variety of MEMS applications both in (Khan et al., 2011; Wang et al., 2007) and out (Bogue, 2016) of the biomedical field. Unlike diamond, it can be synthesized in large single crystals and used in place of silicon as the substrate upon which the devices are built. Diamond, on the other hand, is deposited in a dense conformal layer of crystals only 3–5 nanometers across using chemical vapor deposition techniques common to MEMS processing. It is being investigated as an encapsulating material, deposited over a completed device to hermetically and electrically seal it. Conformal ultrananocrystalline diamond (UNCD) appears chemically inert *in vivo* and its deposition has been optimized to minimize deposition temperature (down to 400 °C), leakage current, and various measures of biocompatibility (Tien et al., 2017; Xiao et al., 2006). *In vitro*, UNCD surfaces show lower macrophage adhesion than polystyrene, with downregulated cytokine production as well (Chen et al., 2014). *In vivo* trials show reduced acute inflammatory response and thinner fibrous capsule formation *vs*. Si, Ti, and Ti/Al alloy (Chen et al., 2014). UNCD can also be doped to form an electrically conductive surface for electrodes, with less *in vivo* fibrous capsule formation than undoped UNCD or silicone (Garrett et al., 2016).

3.4. Fouling

While safety and durability are critical for any medical implant, biosensors and drug delivery systems face added challenges that have

limited them to a tiny fraction of the implant market (24/7Wall St.com, 2011; Darouiche, 2004). In particular, they are susceptible to fouling and encapsulation by the body. Mechanical implants (*e.g.*, bone pins, artificial joints) can supply mechanical support regardless of the presence of biological deposits, and currently account for the lion's share of medical implant market, while another 20 percent of devices provide electrical stimulation (*e.g.* pacemakers, defibrillators) and can detect increases in external resistance, ramping up their electrical potential accordingly to maintain current. Devices which sense chemical signals within the body, however, rely on the assumption that the signal they detect is representative of the body as a whole, either directly or through an established calibration. This is rarely the case over a sustained (> 1 week) period of time (US-FDA, 2016a,b,c), however, though one fully implanted sensor is approved for 90-day use in Europe (Dehennis et al., 2015; Sensionics, 2017). Moreover, only in the past year has one sensor been approved for automated insulin dosing decisions (US-FDA, 2016a), finally providing (partially) closed-loop drug delivery. These limitations are due to a chain of physiological responses to the implant which progressively alter the signal between the body and the sensor. The most immediate of these responses is fouling (Thomé-Duret et al., 1996; Wisniewski et al., 2000), an accumulation of molecules (primarily proteins) and cells on the surface of the device.

Fouling may irreversibly damage the device in a manner similar to corrosion, it may interfere with the device's transduction mechanism, it may interfere with diffusion of the signal (*e.g.*, analyte molecules) to the transduction mechanism, or, in the case of adhered cells, it may form a reactive sink for the signal (*e.g.*, consuming glucose before it is sensed) (Wilson and Gifford, 2005). BioMEMS technology offers several avenues for partially mitigating these problems, however. Fouling, particularly cell attachment, is associated with acute inflammation, the first of two broad phases of the physiological response to sensor implantation. The magnitude of the acute inflammation has been correlated to the magnitude of the implantation trauma, *i.e.*, the size of the implantation incision(Szarowski et al., 2003; Wang et al., 2015). By miniaturizing the device, the size of the implantation incision may be reduced to a needle stick (Liu et al., 2015), minimizing the inducement of inflammation around the device. Conversely, rather than shrinking the size of the device with a single sensor, one may shrink the size of the sensor and incorporate several into the same device(Machado et al., 2016), either to increase the signal-noise ratio or to address heterogeneities at the implant location(Gifford, 2013). MEMS fabrication is particularly well-suited not just to miniaturization but also to extreme replicability for such arrays.

Most ambitiously, one can use MEMS fabrication technology to build membranes with precise pore geometries which will allow the passage of small molecule analytes while blocking larger immunoproteins and cells. For instance, Fig. 8 shows a silicon membrane with slit-shaped pores 7 nm wide above a cavity into which pancreatic islet cells can be held (Leoni et al., 2002; Schweicher et al., 2014). By immunoisolating the islets, these membranes effectively formed a completely internal closed-loop glucose sensor / insulin delivery system. Glucose could enter the device and trigger production of insulin which could leave the device, while blocking immunoresponsive proteins from reaching the islets. Among the problems with that fabrication approach, however, was the low porosity (< < 1%) of the membrane. Alternatively, block copolymers have been used to fabricate membranes with precisely-controlled nanoscale pores at far higher pore density by incorporating the polymer on a microfabricated silicon support with its own high-density array of precisely controlled microscale pores to permit rapid, direct mass transport of small molecules while blocking macromolecules, as shown in Fig. 9 (Nuxoll et al., 2009). The same principle can be applied to protect electrode surfaces from protein fouling either by making the electrode itself porous (Matharu et al., 2017), or by applying a porous material such as mesoporous silica (Serrano et al., 2015) or a polymer hydrogel (Marquez et al., 2017). The latter can also be used to immobilize enzymes needed

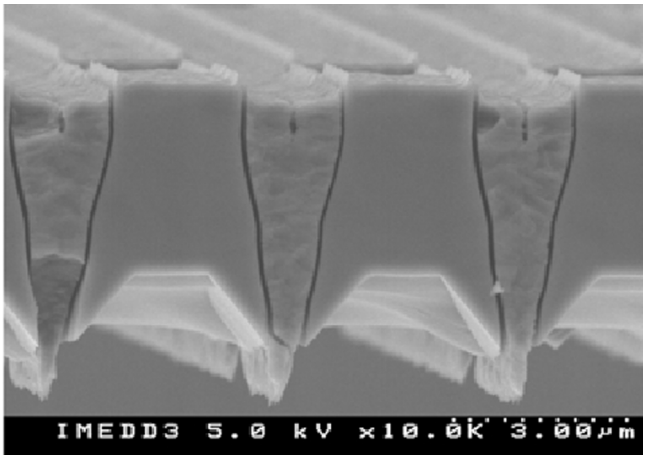

Fig. 8. Microfabricated Silicon Membrane for Immunisolation of Pancreatic Islet Cells. SEM micrograph reproduced with permission from Leoni et al. (2002).

to transduce the chemical signal while similarly protecting them from external proteins (Marquez et al., 2017). Polymers with degradable regions can also be used to generate porosity *in situ* (Vaddiraju et al., 2012), while simultaneously applying another approach to inflammation mitigation: delivery of anti-inflammatory drugs.

Controlled release of anti-inflammatory drugs such as dexamethasone (Dex) has already been demonstrated to stall inflammation and extend the longevity of conventional transcutaneous glucose sensors. Highly microporous polyurethane coatings allowed rapid glucose transport with local Dex delivery, permitting accurate *in vivo* glucose sensing for three weeks(Vallejo-Heligon et al., 2016). Broader tuning of Dex release has been achieved by loading it in degradable poly(lactic-co-glycolic acid) (PLGA) microspheres within a hydrogel matrix of poly (vinyl alcohol (PVA)(Gu et al., 2015; Wang et al., 2013) or collagen(Ju et al., 2010). While Dex effectively stalls the physiological response to the implanted sensor, it does not eliminate it; as soon as the Dex runs out, the sensor is encapsulated(Gu et al., 2015; Norton et al., 2007). This is noteworthy for BioMEMS sensors, as decreasing the device size may decrease its drug loading capacity on a steeper scale than its drug requirement. The ease of integration with additional components provides other avenues for MEMS devices to control drug release, however. By loading Dex into a conducting polymer on a flexible microelectrode, Dex was actively released weekly to maintain steady neural contact for 12 weeks(Boehler et al., 2017). One complication of Dex has been its inhibition of angiogenesis, leaving the sensor more isolated from the bloodstream and more susceptible to encapsulation (Norton et al., 2007). Co-release with L-Dopa has recently demonstrated restored angiogenesis *in vivo* (Price et al., 2016), but it is still not clear that sensor lifetime can be extended beyond the period of Dex release. Similarly, NO has been demonstrated to reduce inflammation *in vivo* when released from silica nanoparticles in a polyurethane coating, but again its effects scale with dose(Nichols et al., 2012; Soto et al., 2017).

3.5. Foreign body response

The greatest barrier (literally) to biosensors is fibrous encapsulation formed as the chronic response to an implanted material(Wisniewski et al., 2001). The evolution of the device site from the moment of implantation through acute inflammation to chronic encapsulation has been reviewed repeatedly and in depth as understanding of this process increases(Bryers et al., 2012; Franz et al., 2011; Helton et al., 2011; Klopfleisch and Jung, 2017; Wilson and Gifford, 2005). The process begins almost instantaneously upon implantation with protein adsorption to the surface. Besides fouling the surface, this adsorption leads to recruitment of macrophages which then differentiate to either drive (M1) or quell (M2) inflammation. Once the macrophages fail to

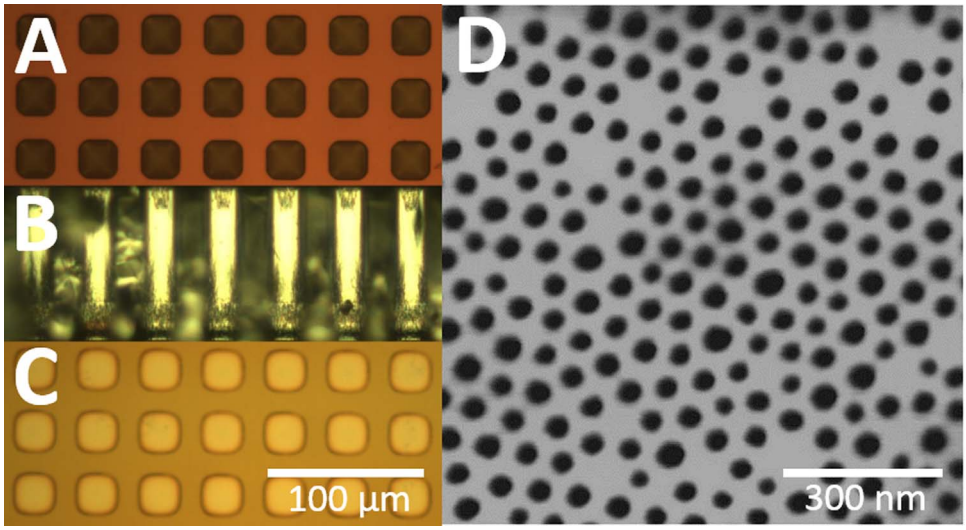

Fig. 9. Composite Block-Copolymer / Microfabricated Silicon Nanoporous Membrane. Microporous silicon support as viewed from the top (A), cross section (B), and bottom (C). Tapping-mode AFM height image of a nanoporous block polymer film on Si_3N_4. Pore diameters are 43 nm ± 11% RSD. Reproduced with permission from Nuxoll et al (2009).

phagocytose the device, they prompt the formation of a fibrous collagen capsule around the device, isolating it from the rest of the body. This capsule creates significant transport resistance between the body and the device, substantially weakening the chemical signal from the body. Moreover, the degree of weakening changes as the capsule is formed, forcing repeated recalibration.

Substantial effort has been devoted to developing surfaces which avoid protein and cell adhesion, not just to avoid fouling as discussed above, but to dodge the larger issue of encapsulation. These approaches often involve surface modification with hydrophilic (*e.g.* poly(ethylene glycol) (Kingshott and Griesser, 1999; Park and McShane, 2010)), zwitterionic (Wang et al., 2017c) (*e.g.* poly(carboxybetaine) (Zhang et al., 2013)), and/or endogenous (*e.g.* basement membrane (Klueh et al., 2015)) macromolecules and can be adapted to many MEMS materials fairly readily. Modifications to switch hydrophilicity for self-cleaning have also been developed (Gant et al., 2010; Gant et al., 2009), as well as modifications for controlled release of drugs which affect macrophage behavior, such as masitinib (Avula et al., 2013), linoleic acids (Pholpabu et al., 2016), apyrase and minocycline (Hayn et al., 2017).

There has also been significant work in altering the topography of the surface, both to manipulate the differentiation of the macrophages (Singh et al., 2017) and to induce vascularization of the surface. While conventional tissue scaffolds use non-woven fiber mats of various materials and growth factors, scaffolds with well-defined fused-sphere pores have been shown to prompt significantly less M1 differentiation and therefore much better vascularization *in vivo*, regardless of chemical modifications (Bryers et al., 2012; Sussman et al., 2014). The precise, ordered, widespread control of micron-scale features at an interface plays directly to the strengths of MEMS technology, which has been used to fabricate 50 µm thick silicon membranes as shown in Fig. 10, prevascularized (Worthington et al., 2016) for facilitating capillary blood flow to within nanometers of any underlying sensor, potentially immunoisolated using the block copolymer approach from Fig. 9.

Even if fibrous encapsulation cannot be completely sidestepped by integrating capillary beds into the device surface, bioMEMS sensors benefit from a basic correlation between device size and degree of encapsulation. Several studies have indicated that smaller implants prompt thinner capsules (Helton et al., 2011; Sommakia et al., 2014; Szarowski et al., 2003; Wang et al., 2015), providing a strong motivation for device miniaturization. However, studies have also indicated that large mismatches between the mechanical moduli of the device and the surrounding tissue prompt greater encapsulation (Helton et al., 2011; Lee et al., 2017; Sommakia et al., 2014). Traditional MEMS materials such as silicon and sapphire are many orders of magnitude harder than tissue, but these fabrication processes have been adapted to more flexible materials such as polyimide. Flexible polyimide neural probes have exhibited significantly less foreign body response, though this may be in part due to less micromotion at the probe surface from jostling of the transcutaneous electrical connections (Sohal et al., 2016). Many MEMS devices are also made *via* soft lithography, where traditional lithography is used to fabricate a negative master mold of the desired shape. Poly(dimethyl siloxane) (PDMS) is then poured over the mold and cured, forming a soft rubbery substrate with precisely patterned submicron features. While substantially less encapsulation was observed for devices made of PDMS rather than silicon, little improvement was seen by moving to even softer materials which would be difficult to process with MEMS technology (Lee et al., 2017).

4. Summary

MEMS technologies are integral to the growth of biosensing, particularly for chemical signals within the body. The small size of MEMS devices gives them access to previously inaccessible locations while minimizing the discomfort to the patient. Their small size also minimizes their power consumption and reduces the time required for chemical analytes to diffuse throughout the sensing medium, though it also reduces the opportunity for light to interact with the analyte in direct optical sensing. Studies also indicate that the Achilles heel of implantable chemical sensing, fibrous encapsulation, decreases with decreased device size, and approaches to preventing or bypassing encapsulation using the exquisite geometrical control of MEMS fabrication are currently under investigation. MEMS manufacturing processes, refined by decades of use in the computer industry, provide scalable production with extremely high reproducibility and reliability. Moreover, this format is already used for making the control circuits, telemetry, and dosing devices to which the sensor must interface, facilitating seamless integration of these components not just for reporting but also for closed-loop drug delivery. A wide variety of sensing mechanisms have been developed, several of which are already in clinical use. These include glucose sensors which combine the high substrate selectivity of enzymes with the high sensitivity of electrochemical measurements, as well as optical glucose sensors and capacitive pressure sensors for a variety of indications, with many more devices under development.

Acknowledgments

This work was supported in part by the National Science Foundation

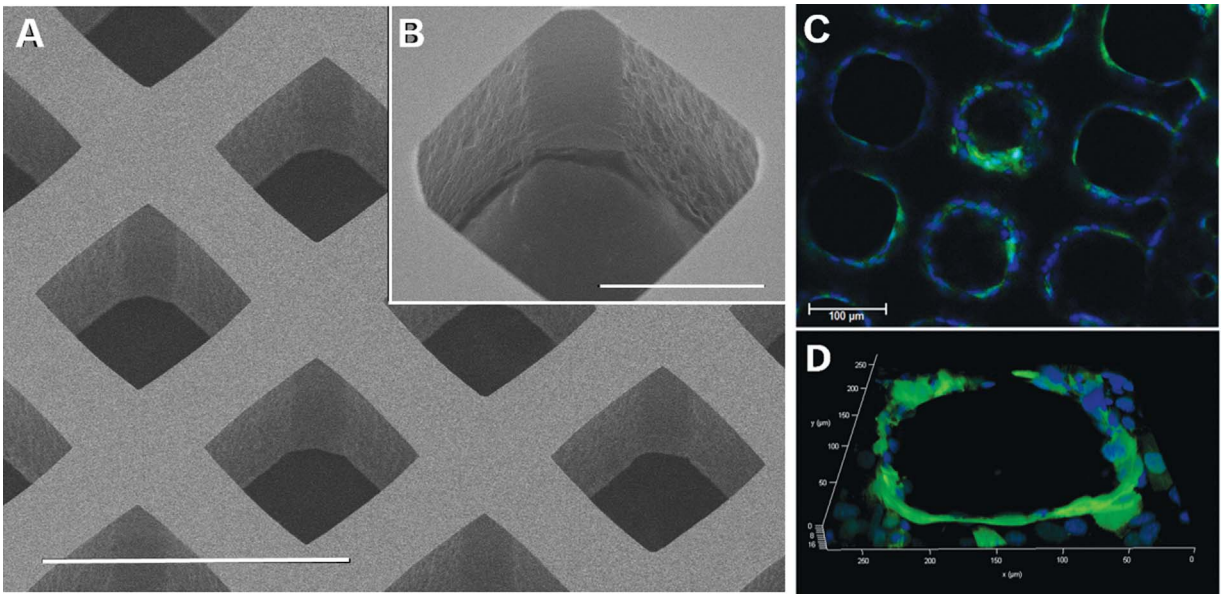

Fig. 10. Prevascularized Silicon Membranes for the Enhancement of Transport to Implanted Medical Devices. A) SEM micrograph of 50 µm-thick silicon membrane with array of pores, magnified in inset (B). C) Murine vascular endothelial cells form ring structures around pores, shown in 3-D in panel (D). Reproduced with permission from Worthington et al. (2016).

(CBET-1133297) and the American Heart Association (11SDG7600044).

References

24/7 Wall St.com, 2011. The Eleven Most Implanted Medical Devices in America. http://247wallst.com/healthcare-economy/2011/07/18/the-eleven-most-implanted-medical-devices-in-america/. Accessed 10 April 2015. .

Abraham, W.T., Adamson, P.B., Bourge, R.C., Aaron, M.F., Costanzo, M.R., Stevenson, L.W., Strickland, W., Neelagaru, S., Raval, N., Krueger, S., Weiner, S., Shavelle, D., Jeffries, B., Yadav, J.S., 2011. Wireless pulmonary artery haemodynamic monitoring in chronic heart failure: a randomised controlled trial. Lancet 377, 658–666.

Allied Market Research, 2016. Global continuous glucose monitoring systems market by components, demographics, and end users. Global Oppor. Anal. Ind. Forecast 2014–2022, 203.

Apigo, D.J., Bartholomew, P.L., Russell, T., Kanwal, A., Farrow, R.C., Thomas, G.A., 2016. An angstrom-sensitive, differential MEMS capacitor for monitoring the milliliter dynamics of fluids. Sens. Actuators A Phys. 251, 234–240.

Avula, M.N., Rao, A.N., McGill, L.D., Grainger, D.W., Solzbacher, F., 2013. Modulation of the foreign body response to implanted sensor models through device-based delivery of the tyrosine kinase inhibitor, masitinib. Biomaterials 34, 9737–9746.

Badilescu, S., Muthukumaran, P., 2011. BioMEMS Science and Engineering Perspectives. CRC Press, Boca Raton, FL.

Baldi, A., Lei, M., Gu, Y., Siegel, R.A., Ziaie, B., 2006. A microstructured silicon membrane with entrapped hydrogels for environmentally sensitive fluid gating. Sens. Actuators B 114, 9–18.

Balslev, S., Jorgensen, A.M., Bilenberg, B., Mogensen, K.B., Snakenborg, D., Geschke, O., Kutter, J.P., Kristensen, A., 2006. Lab-on-a-chip with integrated optical transducers. Lab Chip 6, 213–217.

Barsan, M.M., Ghica, M.E., Brett, C.M., 2015. Electrochemical sensors and biosensors based on redox polymer/carbon nanotube modified electrodes: a review. Anal. Chim. Acta 881, 1–23.

Bashir, R., Wereley, S., 2006. Biomolecular sensing, processing and analysis. In: Ferrari, M. (Ed.), BioMEMS and Biomedical Nanotechnology. Springer, New York, NY, pp. 407.

Bayer, C.L., Peppas, N.A., 2008. Advances in recognitive, conductive and responsive delivery systems. J. Control. Release 132, 216–221.

Bhatnagar, S., Dave, K., Venuganti, V.V.K., 2017. Microneedles in the clinic. J. Control. Release 260, 164–182.

Birkholz, M., Ehwald, K.E., Basmer, T., Kulse, P., Reich, C., Drews, J., Genschow, D., Haak, U., Marschmeyer, S., Matthus, E., Schulz, K., Wolansky, D., Winkler, W., Guschauski, T., Ehwald, R., 2013. Sensing glucose concentrations at GHz frequencies with a fully embedded biomicro-electromechanical system (BioMEMS). J. Appl. Phys. 113, 244904.

Birkholz, M., Glogener, P., Glös, F., Basmer, T., Theuer, L., 2016. Continuously operating biosensor and its integration into a hermetically sealed medical implant. Micromachines 7, 183.

Boehler, C., Kleber, C., Martini, N., Xie, Y., Dryg, I., Stieglitz, T., Hofmann, U.G., Asplund, M., 2017. Actively controlled release of dexamethasone from neural microelectrodes in a chronic in vivo study. Biomaterials 129, 176–187.

Bogue, R., 2016. Non-silicon MEMS – the hard and soft alternatives. Sens. Rev. 36, 225–230.

Brahim, S., Wilson, A.M., Narinesingh, D., Iwuoha, E., Guiseppi-Elie, A., 2003. Chemical and biological sensors based on electrochemical detection using conducting electroactive polymers. Microchim. Acta 143, 123–137.

Bryers, J.D., Giachelli, C.M., Ratner, B.D., 2012. Engineering biomaterials to integrate and heal: the biocompatibility paradigm shifts. Biotechnol. Bioeng. 109, 1898–1911.

Cadarso, V.J., Llobera, A., Puyol, M., Schift, H., 2016. Integrated photonic nanofences: combining subwavelength waveguides with an enhanced evanescent field for sensing applications. ACS Nano 10, 778–785.

Cadei, A., Dionisi, A., Sardini, E., Serpelloni, M., 2014. Kinetic and thermal energy harvesters for implantable medical devices and biomedical autonomous sensors. Meas. Sci. Technol. 25, 012003.

Cao, H., Landge, V., Tata, U., Seo, Y.-S., Rao, S., Tang, S.-J., Tibbals, H.F., Spechler, S., Chiao, J.-C., 2012. An implantable, batteryless, and wireless capsule with integrated impedance and pH sensors for gastroesophageal reflux monitoring. IEEE Trans. Biomed. Eng. 59, 3131–3139.

Castanheiro, J.E., Ramos, A.M., Fonseca, I.M., Vital, J., 2006. Esterification of acetic acid by isoamylic alcohol over catalytic membranes of poly(vinyl alcohol) containing sulfonic acid groups. Appl. Catal. A 311, 17–23.

Castro, P.F., Concepcion, R., Bourge, R.C., Martinez, A., Alcaino, M., Deck, C., Ferrada, M., Alfaro, M., Perrone, S., 2007. A wireless pressure sensor for monitoring pulmonary artery pressure in advanced heart failure: initial experience. J. Heart Lung Transpl. 26, 85–88.

Chang, C.P., Nagel, D.J., Velasquez, M.T., Zaghloul, M.E., 2011. Compact optical microfluidic uric acid analysis system. Biosens. Bioelectron. 26, 4155–4161.

Chen, A., Chatterjee, S., 2013. Nanomaterials based electrochemical sensors for biomedical applications. Chem. Soc. Rev. 42, 5425–5438.

Chen, P.-J., Saati, S., Varma, R., Humayun, M.S., Tai, Y.-C., 2010. Wireless intraocular pressure sensing using microfabricated minimally invasive flexible-coiled LC sensor implant. J. Microelectromech. Syst. 19, 721–734.

Chen, Y.C., Tsai, C.Y., Lee, C.Y., Lin, I.N., 2014. In vitro and in vivo evaluation of ultrananocrystalline diamond as an encapsulation layer for implantable microchips. Acta Biomater. 10, 2187–2199.

Chia, X., Eng, A.Y., Ambrosi, A., Tan, S.M., Pumera, M., 2015. Electrochemistry of nanostructured layered transition-metal dichalcogenides. Chem. Rev. 115, 11941–11966.

Chikkaveeraiah, B.V., Liu, H., Mani, V., Papadimitrakopoulos, F., Rusling, J.F., 2009. A microfluidic electrochemical device for high sensitivity biosensing: detection of nanomolar hydrogen peroxide. Electrochem. Commun. 11, 819–822.

Chow, E.Y., Chlebowski, A.L., Chakraborty, S., Chappell, W.J., Irazoqui, P.P., 2010. Fully wireless implantable cardiovascular pressure monitor integrated with a medical stent. IEEE Trans. Bio-Med. Eng. 57, 1487–1496.

Coffel, J., Gandhi, S., Nuxoll, E., 2016. Unified polymer erosion model for pulsatile drug delivery. J. Membr. Sci. 512, 61–72.

Colvin, A.E., Jiang, H., 2013. Increased in vivo stability and functional lifetime of an implantable glucose sensor through platinum catalysis. J. Biomed. Mater. Res. Part A 101, 1274–1282.

Costanzo, M.R., Stevenson, L.W., Adamson, P.B., Desai, A.S., Heywood, J.T., Bourge, R.C., Bauman, J., Abraham, W.T., 2016. Interventions linked to decreased heart failure hospitalizations during ambulatory pulmonary artery pressure monitoring. JACC Heart Fail. 4, 333–344.

Courtland, R., 2017. Intel now packs 100 million transistors in each square millimeter.

IEEE Spectr. IEEE.
Darouiche, R.O., 2004. Treatment of infections associated with surgical implants. N. Eng. J. Med. 350, 1422–1429.
Dehennis, A., Mortellaro, M.A., Ioacara, S., 2015. Multisite study of an implanted continuous glucose sensor over 90 days in patients with diabetes mellitus. J. Diabetes Sci. Technol. 9, 951–956.
Deng, K., Bellmann, C., Fu, Y., Rohn, M., Guenther, M., Gerlach, G., 2018. Miniaturized force-compensated hydrogel-based pH sensors. Sens. Actuators B: Chem. 255, 3495–3504.
Do, U.P., Seland, F., Maharbiz, M.M., Wang, K., Johannesen, Ø., Johannessen, E.A., 2016. Thin film nanoporous electrodes for the selective catalysis of oxygen in abiotically catalysed micro glucose fuel cells. J. Mater. Sci. 51, 9095–9107.
Eddington, D., Beebe, D., 2004. Flow control with hydrogels. Adv. Drug Deliv. Rev. 56, 199–210.
Esfandyarpour, R., Esfandyarpour, H., Harris, J.S., Davis, R.W., 2013. Simulation and fabrication of a new novel 3D injectable biosensor for high throughput genomics and proteomics in a lab-on-a-chip device. Nanotechnology 24, 465301.
Farra, R., Sheppard, N.F., McCabe, L., Neer, R.M., Anderson, J.M., Santini, J.T., Cima, M.J., Langer, R., 2012. First-in-human testing of a wirelessly controlled drug delivery microchip. Sci. Transl. Med. 4, 122ra121.
Fernandes, L.A.L., Azadmehr, M., Johannessen, E.A., Hafliger, P., 2016. An osmotic pressure sensor for monitoring the level of hydration in biological fluids. IEEE Sens. J. 16, 4331–4337.
Ferrara, L.A., Fleischman, A.J., Togawa, D., Bauer, T.W., Benzel, E.C., Roy, S., 2003. An in vivo biocompatibility assessment of MEMS materials for spinal fusion monitoring. Biomed. Microdev. 5, 297–302.
Ferri, S., Kojima, K., Sode, K., 2011. Review of glucose oxidases and glucose dehydrogenases: a bird's Eye view of glucose sensing enzymes. J. Diabetes Sci. Technol. 5, 1068–1076.
Ferrier, D.C., Shaver, M.P., Hands, P.J., 2015. Micro- and nano-structure based oligonucleotide sensors. Biosens. Bioelectron. 68, 798–810.
Finkle, J., 2016. J&J Warns Diabetic Patients: Insulin Pump Vulnerable to Hacking. Reuters. .
Folch, A., 2012. Introduction to BioMEMS, 1st ed. CRC Press.
Franz, S., Rammelt, S., Scharnweber, D., Simon, J.C., 2011. Immune responses to implants–a review of the implications for the design of immunomodulatory biomaterials. Biomaterials 32, 6692–6709.
French, M.T., Homer, J., Gumus, G., Hickling, L., 2016. Key provisions of the patient protection and Affordable Care Act (ACA): a systematic review and presentation of early research findings. Health Serv. Res. 51, 1735–1771.
Gant, R.M., Abraham, A.A., Hou, Y., Cummins, B.M., Grunlan, M.A., Cote, G.L., 2010. Design of a self-cleaning thermoresponsive nanocomposite hydrogel membrane for implantable biosensors. Acta Biomater. 6, 2903–2910.
Gant, R.M., Hou, Y., Grunlan, M.A., Cote, G.L., 2009. Development of a self-cleaning sensor membrane for implantable biosensors. J. Biomed. Mater. Res. Part A 90, 695–701.
Garrett, D.J., Saunders, A.L., McGowan, C., Specks, J., Ganesan, K., Meffin, H., Williams, R.A., Nayagam, D.A., 2016. In vivo biocompatibility of boron doped and nitrogen included conductive-diamond for use in medical implants. J. Biomed. Mater. Res. B Appl. Biomater. 104, 19–26.
Gawel, K., Barriet, D., Sletmoen, M., Stokke, B.T., 2010. Responsive hydrogels for label-free signal transduction within biosensors. Sensors 10, 4381–4409.
Gencoglu, A., Minerick, A.R., 2014. Electrochemical detection techniques in micro- and nanofluidic devices. Microfluid. Nanofluid. 17, 781–807.
Gifford, R., 2013. Continuous glucose monitoring: 40 years, what we've learned and what's next. Chemphyschem: Eur. J. Chem. Phys. Phys. Chem. 14, 2032–2044.
Gilligan, B.J., Shults, M.C., Rhodes, R.K., Jacobs, P.G., Brauker, J.H., Pintar, T.J., Updike, S.J., 2004. Feasibility of continuous long-term glucose monitoring from a subcutaneous glucose sensor in humans. Diabetes Technol. Ther. 6, 378–386.
Gough, D.A., Kumosa, L.S., Routh, T.L., Lin, J.T., Lucisano, J.Y., 2010. Function of an implanted tissue glucose sensor for more than 1 year in animals. Sci. Transl. Med. 2, ra53.
Griveau, S., Bedioui, F., 2013. Overview of significant examples of electrochemical sensor arrays designed for detection of nitric oxide and relevant species in a biological environment. Anal. Bioanal. Chem. 405, 3475–3488.
Gu, B., Wang, Y., Burgess, D.J., 2015. In vitro and in vivo performance of dexamethasone loaded PLGA microspheres prepared using polymer blends. Int. J. Pharm. 496, 534–540.
Hafezi, H., Robertson, T.L., Moon, G.D., Au-Yeung, K.-Y., Zdeblick, M.J., Savage, G.M., 2015. An ingestible sensor for measuring medication adherence. IEEE Trans. Biomed. Eng. 62, 99–109.
Hämmerle, H., Kobuch, K., Kohler, K., Nisch, W., Sachs, H., Stelzle, M., 2002. Biostability of micro-photodiode arrays for subretinal implantation. Biomaterials 23, 797–804.
Hayn, L., Deppermann, L., Koch, M., 2017. Reduction of the foreign body response and neuroprotection by apyrase and minocycline in chronic cannula implantation in the rat brain. Clin. Exp. Pharmacol. Physiol. 44, 313–323.
Helton, K.L., Ratner, B.D., Wisniewski, N.A., 2011. Biomechanics of the sensor–tissue interface—effects of motion, pressure, and design on sensor performance and the foreign body response—part I: theoretical framework. J. Diabetes Sci. Technol. 5, 632–646.
Hilt, J.Z., Gupta, A.K., Bashir, R., Peppas, N.A., 2003. Ultrasensitive biomems sensors based on microcantilevers patterned with environmentally responsive hydrogels. Biomed. Microdevices 5, 177–184.
Hilt, J.Z., Peppas, N.A., 2005. Microfabricated drug delivery devices. Int. J. Pharm. 306, 15–23.
Hirokawa, Y., Tanaka, T., 1984. Volume phase transition in a nonionic gel. J. Chem. Phys. 81, 6379–6380.
Hirotsu, S., Hirokawa, Y., Tanaka, T., 1987. Volume-phase transitions of ionized N-isopropylacrylamide gels. J. Chem. Phys. 87, 1392–1395.
Huang, W.-D., Cao, H., Deb, S., Chiao, M., Chiao, J.C., 2011. A flexible pH sensor based on the iridium oxide sensing film. Sens. Actuators A: Phys. 169, 1–11.
Irawan, R., Tjin, S.C., Fang, X., Fu, C.Y., 2007. Integration of optical fiber light guide, fluorescence detection system, and multichannel disposable microfluidic chip. Biomed. Microdevices 9, 413–419.
Jin, J., Sanchez-Sinencio, E., 2015. A home sleep apnea screening device with time-domain signal processing and autonomous scoring capability. IEEE Trans. Biomed. Circuits Syst. 9, 96–104.
Jochum, F.D., Theato, P., 2013. Temperature- and light-responsive smart polymer materials. Chem. Soc. Rev. 42, 7468–7483.
Ju, Y.M., Yu, B., West, L., Moussy, Y., Moussy, F., 2010. A dexamethasone-loaded PLGA microspheres/collagen scaffold composite for implantable glucose sensors. J. Biomed. Mater. Res. Part A 93, 200–210.
Kabilan, S., Marshall, A.J., Sartain, F.K., Lee, M.C., Hussain, A., Yang, X., Blyth, J., Karangu, N., James, K., Zeng, J., Smith, D., Domschke, A., Lowe, C.R., 2005. Holographic glucose sensors. Biosens. Bioelectron. 20, 1602–1610.
Kanekiyo, Y., Sano, M., Iguchi, R., Shinkai, S., 2000. Novel nucleotide-responsive hydrogels designed from copolymers of boronic acid and cationic units and their applications as a QCM resonator system to nucleotide sensing. J. Polym. Sci.: Part A: Polym. Chem. 38, 1302–1310.
Kataoka-Hamai, C., Miyahara, Y., 2011. Label-free detection of DNA by field-effect devices. IEEE Sens. J. 11, 3153–3160.
Kataoka, K., Miyazaki, H., Bunya, M., Okano, T., Sakurai, Y., 1998. Totally synthetic polymer gels responding to external glucose concentration: their preparation and application to on-off regulation of insulin release. J. Am. Chem. Soc. 120, 12694–12695.
Kawoos, U., Tofighi, M.R., Warty, R., Kralick, F.A., Rosen, A., 2008. In-vitro and in-vivo trans-scalp evaluation of an intracranial pressure implant at 2.4 GHz. IEEE Trans. Microw. Theory Techn. 56, 2356–2365.
Khan, S.P., Auner, G.G., Palyvoda, O., Newaz, G.M., 2011. Biocompatibility assessment of next generation materials for brain implantable microelectrodes. Mater. Lett. 65, 876–879.
Kim, Y.-C., Park, J.-H., Prausnitz, M.R., 2012. Microneedles for drug and vaccine delivery. Adsorpt. Sci. Technol. 64, 1547–1568.
Kim, Y.T., Kim, Y.-Y., Jun, C.-H., 1999. Needle-shaped glucose sensor with multicell electrode fabricated by surface micromachining. Proc. SPIE 3680, 924–930.
Kingshott, P., Griesser, H.J., 1999. Surfaces that resist bioadhesion. Curr. Opin. Solid State Mater. Sci. 4, 403–412.
Klopfleisch, R., Jung, F., 2017. The pathology of the foreign body reaction against biomaterials. J. Biomed. Mater. Res. Part A 105, 927–940.
Klouda, L., 2015. Thermoresponsive hydrogels in biomedical applications: A seven-year update. Eur. J. Pharm. Biopharm.: Off. J. Arbeitsgemeinschaft fur Pharmazeutische Verfahrenstechnik e.V 97, 338–349.
Klueh, U., Qiao, Y., Czajkowski, C., Ludzinska, I., Antar, O., Kreutzer, D.L., 2015. Basement membrane-based glucose sensor coatings enhance continuous glucose monitoring in vivo. J. Diabetes Sci. Technol. 9, 957–965.
Koçak, Y., Akaltun, Y., Gür, E., 2016. Magnetron sputtered WS 2 ; optical and structural analysis. J. Phys.: Conf. Ser. 707, 012028.
Kotzar, G., Freas, M., Abel, P., Fleischman, A., Roy, S., Zorman, C., Moran, J.M., Melzak, J., 2002. Evaluation of MEMS materials of construction for implantable medical devices. Biomaterials 23, 2737–2750.
Kumosa, L.S., Routh, T.L., Lin, J.T., Lucisano, J.Y., Gough, D.A., 2014. Permeability of subcutaneous tissues surrounding long-term implants to oxygen. Biomaterials 35, 8287–8296.
Kuo, C.N., Lin, P.C., Campo, F.J.D., Tsai, Y.C., 2015. Construction of a hydrogen peroxide biosensor on interdigitated microband electrodes fabricated by a mix-and-match process. J. Electrochem. Soc. 162, B133–B137.
Kwiatek, M.A., Pandolfino, J.E., 2007. Prolonged reflux monitoring: capabilities of bravo pH and impedance-pH systems. Curr. GERD Rep. 1, 165–170.
Lai, W.A., Lin, C.H., Yang, Y.S., Lu, M.S., 2012. Ultrasensitive and label-free detection of pathogenic avian influenza DNA by using CMOS impedimetric sensors. Biosens. Bioelectron. 35, 456–460.
Lambeck, P.V., 2006. Integrated optical sensors for the chemical domain. Meas. Sci. Technol. 17, R93–R116.
Larraneta, E., McCrudden, M.T., Courtenay, A.J., Donnelly, R.F., 2016. Microneedles: a new frontier in nanomedicine delivery. Pharm. Res. 33, 1055–1073.
Lee, C.-S., Kim, S.K., Kim, M., 2009. Ion-sensitive field-effect transistor for biological sensing. Sensors (Basel, Switzerland) 9, 7111–7131.
Lee, H.C., Ejserholm, F., Gaire, J., Currlin, S., Schouenborg, J., Wallman, L., Bengtsson, M., Park, K., Otto, K.J., 2017. Histological evaluation of flexible neural implants; flexibility limit for reducing the tissue response? J. Neural Eng. 14, 036026.
Lei, M., Baldi, A., Nuxoll, E., Siegel, R.A., Ziaie, B., 2006. A hydrogel-based implantable micromachined transponder for wireless glucose measurement. Diabetes Technol. Ther. 8, 112–121.
Lei, M., Baldi, A., Nuxoll, E., Siegel, R.A., Ziaie, B., 2009. Hydrogel-based sensors for wireless chemical monitoring. Biomed. Microdevices 11, 529–538.
Lei, M., Ziaie, B., Nuxoll, E., Iván, K., Noszticzius, Z., Siegel, R.A., 2007. Integration of hydrogels with hard and soft microstructures. J. Nanosci. Nanotechnol. 7, 780–789.
Leoni, L., Boiarski, A., Desai, T., 2002. Characterization of nanoporous membranes for immunoisolation: diffusion properties and tissue effects. Biomed. Microdevices 4, 131–139.
Li, C.M., Dong, H., Cao, X., Luong, J.H.T., Zhang, X., 2007. Implantable electrochemical sensors for biomedical and clinical applications: progress, problems, and future

possibilities. Curr. Med. Chem. 14, 937–951.
Li, Y., Tanaka, T., 1990. Kinetics of swelling and shrinking of gels. J. Chem. Phys. 92, 1365–1371.
Liu, J., Fu, T.M., Cheng, Z., Hong, G., Zhou, T., Jin, L., Duvvuri, M., Jiang, Z., Kruskal, P., Xie, C., Suo, Z., Fang, Y., Lieber, C.M., 2015. Syringe-injectable electronics. Nat. Nanotechnol. 10, 629–636.
Llobera, A., Demming, S., Wilke, R., Buttgenbach, S., 2007. Multiple internal reflection poly(dimethylsiloxane) systems for optical sensing. Lab Chip 7, 1560–1566.
Lucisano, J.Y., Routh, T.L., Lin, J.T., Gough, D.A., 2017. Glucose monitoring in individuals with diabetes using a long-term implanted sensor/telemetry system and model. IEEE Trans. Biomed. Eng. 64, 1982–1993.
Luo, M., Martinez, A.W., Song, C., Herrault, F., Allen, M.G., 2014. A microfabricated wireless RF pressure sensor made completely of Biodegradable materials. J. Microelectromech. Syst. 23, 4–13.
Machado, R., Soltani, N., Dufour, S., Salam, M.T., Carlen, P.L., Genov, R., Thompson, M., 2016. Biofouling-resistant impedimetric sensor for array high-Resolution extracellular potassium monitoring in the brain. Biosensors 6.
Madou, M.J., 2011. Fundamentals of Microfabrication and Nanotechnology, 3rd ed. CRC Press, Boca Raton.
Maloney, J.M., Lipka, S.A., Baldwin, S.P., 2005. In vivo biostability of CVD silicon oxide and silicon nitride films. MRS Symp. Proc. 872, J14.
MarketsandMarkets, 2017. Biosensors Market - Global Forecast to 2022. pp. 182.
Marquez, A., Jimenez-Jorquera, C., Dominguez, C., Munoz-Berbel, X., 2017. Electrodepositable alginate membranes for enzymatic sensors: an amperometric glucose biosensor for whole blood analysis. Biosens. Bioelectron. 97, 136–142.
Matharu, Z., Daggumati, P., Wang, L., Dorofeeva, T.S., Li, Z., Seker, E., 2017. Nanoporous-gold-based electrode morphology libraries for investigating structure-property relationships in nucleic acid based electrochemical biosensors. ACS Appl. Mater. Interfaces 9, 12959–12966.
McKean, B.D., Gough, D.A., 1988. A telemetry-instrumentation system for chronically implanted glucose and oxygen sensors. IEEE Trans. Biomed. Eng. 35, 526–532.
Miyata, T., Asami, N., Uragami, T., 1999. A reversibly antigen-responsive hydrogel. Nature 399, 766–769.
Mortellaro, M., DeHennis, A., 2014. Performance characterization of an abiotic and fluorescent-based continuous glucose monitoring system in patients with type 1 diabetes. Biosens. Bioelectron. 61, 227–231.
Muscatello, M.M.W., Stunja, L.E., Asher, S.A., 2009. Polymerized crystalline colloidal array sensing of high glucose concentrations. Anal. Chem. 81, 4978–4986.
Myers, F.B., Lee, L.P., 2008. Innovations in optical microfluidic technologies for point-of-care diagnostics. Lab Chip 8, 2015–2031.
Nguyen, T., Magda, J.J., Tathireddy, P., 2018. Manipulation of the isoelectric point of polyampholytic smart hydrogels in order to increase the range and selectivity of continuous glucose sensors. Sens. Actuators B: Chem. 255, 1057–1063.
Nichols, S.P., Koh, A., Brown, N.L., Rose, M.B., Sun, B., Slomberg, D.L., Riccio, D.A., Klitzman, B., Schoenfisch, M.H., 2012. The effect of nitric oxide surface flux on the foreign body response to subcutaneous implants. Biomaterials 33, 6305–6312.
Norton, L.W., Koschwanez, H.E., Wisniewski, N.A., Klitzman, B., Reichert, W.M., 2007. Vascular endothelial growth factor and dexamethasone release from nonfouling sensor coatings affect the foreign body response. J. Biomed. Mater. Res. Part A 81, 858–869.
Nuxoll, E., 2013. BioMEMS in drug delivery. Adv. Drug Deliv. Rev. 65, 1611–1625.
Nuxoll, E.E., Hillmyer, M.A., Wang, R., Leighton, C., Siegel, R.A., 2009. Composite block polymer-microfabricated silicon nanoporous membrane. ACS Appl. Mater. Interfaces 1, 888–893.
Ozeri, S., Shmilovitz, D., 2010. Ultrasonic transcutaneous energy transfer for powering implanted devices. Ultrasonics 50, 556–566.
P&S Market Research, 2016. Global Biosensors Market Size, Share, Development, Growth and Demand Forecast to 2022. pp. 116.
Park, J., McShane, M.J., 2010. Dual-function nanofilm coatings with diffusion control and protein resistance. ACS Appl. Mater. Interfaces 2, 991–997.
Peppas, N.A., Van Blarcom, D.S., 2016. Hydrogel-based biosensors and sensing devices for drug delivery. J. Control. Release 240, 142–150.
Pholpabu, P., Yerneni, S.S., Zhu, C., Campbell, P.G., Bettinger, C.J., 2016. Controlled release of small molecules from elastomers for reducing epidermal downgrowth in percutaneous devices. ACS Biomater. Sci. Eng. 2, 1464–1470.
Pilcher, J., Beasley, R., 2015. Acute use of oxygen therapy. Aust. Prescr. 38, 98–100.
Price, C.F., Burgess, D.J., Kastellorizios, M., 2016. l-DOPA as a small molecule surrogate to promote angiogenesis and prevent dexamethasone-induced ischemia. J. Control. Release 235, 176–181.
Prioleau, T., Moore, E., Ghovanloo, M., 2017. Unobtrusive andWearable systems for automatic dietary monitoring. IEEE Trans. Biomed. Eng. 64, 2075–2089.
Ren, H., Coughlin, M.A., Major, T.C., Aiello, S., Rojas Pena, A., Bartlett, R.H., Meyerhoff, M.E., 2015. Improved in vivo performance of amperometric oxygen (PO2) sensing catheters via electrochemical nitric oxide generation/release. Anal. Chem. 87, 8067–8072.
Rodríguez-Ruiz, I., Ackermann, T.N., Muñoz-Berbel, X., Llobera, A., 2016. Photonic lab-on-a-chip: integration of optical spectroscopy in microfluidic systems. Anal. Chem. 88, 6630–6637.
Ruan, C., Zeng, K., Grimes, C.A., 2003. A mass-sensitive pH sensor based on a stimuli-responsive polymer. Anal. Chim. Acta 497, 123–131.
Sassa, F., Laghzali, H., Fukuda, J., Suzuki, H., 2010. Coulometric detection of components in liquid plugs by microfabricated flow channel and electrode structures. Anal. Chem. 82, 8725.
Sauer, C., Stanaćević, M., Cauwenberghs, G., Thakor, N., 2005. Power harvesting and telemetry in CMOS for implanted devices. IEEE Trans. Circuits Syst. 52, 2605–2613.
Schmelzeisen-Redeker, G., Staib, A., Strasser, M., Müller, U., Schoemaker, M., 2013. Overview of a novel sensor for continuous glucose monitoring. J. Diabetes Sci. Technol. 7, 808–814.
Schmitt, G., Schultze, J.-W., Faßbender, F., Buß, G., Lüth, H., Schöning, M.J., 1999. Passivation and corrosion of microelectrode arrays. Electrochim. Acta 44, 3865–3883.
Schweicher, J., Nyitray, C., Desai, T.A., 2014. Membranes to achieve immunoprotection of transplanted islets. Front. Biosci. 19, 49–76.
Sensionics, 2017. http://www.senseonics.com/. Accessed 18 August 2017.
Serrano, M.B., Despas, C., Herzog, G., Walcarius, A., 2015. Mesoporous silica thin films for molecular sieving and electrode surface protection against biofouling. Electrochem. Comm. 52, 34–36.
Siegel, R.A., Firestone, B.A., 1988. pH-dependent equilibrium swelling properties of hydrophobic polyelectrolyte copolymer gels. Macromolecules 21, 3254–3259.
Siegel, R.A., Gu, Y., Li, M., Baldi, A., Nuxoll, E.E., Ziaie, B., 2010. Hard and soft micro- and nanofabrication: an integrated approach to hydrogel based biosensing and drug delivery. J. Control. Release 141, 303–313.
Siegel, R.A., Nuxoll, E.E., Hillmyer, M.A., Ziaie, B., 2009. Top-down and bottom-up fabrication techniques for hydrogel based sensing and hormone delivery microdevices. Proc. Int. Conf. IEEE Eng. Med. Biol. Soc. 31, 232–235.
Singh, S., Awuah, D., Rostam, H.M., Emes, R.D., Kandola, N.K., Onion, D., Htwe, S.S., Rajchagool, B., Cha, B.-H., Kim, D., Tighe, P.J., Vrana, N.E., Khademhosseini, A., Ghaemmaghami, A., 2017. Unbiased analysis of the impact of micropatterned biomaterials on macrophage behavior provides insights beyond predefined polarization states. ACS Biomater. Sci. Eng. 3, 969–978.
Slaughter, G., Kulkarni, T., 2017. Highly selective and sensitive self-powered glucose sensor based on capacitor circuit. Sci. Rep. 7, 1471.
Sohal, H.S., Clowry, G.J., Jackson, A., O'Neill, A., Baker, S.N., 2016. Mechanical flexibility reduces the foreign body response to long-term implanted microelectrodes in rabbit cortex. PLoS One 11, e0165606.
Sommakia, S., Lee, H.C., Gaire, J., Otto, K.J., 2014. Materials approaches for modulating neural tissue responses to implanted microelectrodes through mechanical and biochemical means. Curr. Opin. Solid State Mater. Sci. 18, 319–328.
Song, S.H., Park, J.H., Chitnis, G., Siegel, R.A., Ziaie, B., 2014. A wireless chemical sensor featuring iron oxide nanoparticle-embedded hydrogels. Sens. Actuators B: Chem. 193, 925–930.
Soto, R.J., Schofield, J.B., Walter, S.E., Malone-Povolny, M.J., Schoenfisch, M.H., 2017. Design considerations for silica-particle-doped nitric-oxide-releasing polyurethane glucose biosensor membranes. ACS Sens. 2, 140–150.
Steimle, A.E., Stevenson, L.W., Chelimsky-Fallick, C., Fonarow, G.C., Hamilton, M.A., Moriguchi, J.D., Kartashov, A., Tillisch, J.H., 1997. Sustained hemodynamic efficacy of therapy tailored to reduce filling pressures in survivors with advanced heart failure. Circulation 96, 1165.
Stevenson, L.W., 1999. Tailored therapy to hemodynamic goals for advanced heart failure. Eur. J. Heart Fail. 1, 251–257.
Su, F., Zhang, L., Kong, X., Lee, F., Tian, Y., Meldrum, D.R., 2017. Ratiometric glucose sensing based on fluorescent oxygen films and glucose oxidase. Sens. Bio-Sens. Res. 14, 1–6.
Sumaru, K., Kameda, M., Kanamori, T., Shinbo, T., 2004. Characteristic phase transition of aqueous solution of poly(N-isopropylacrylamide) functionalized with spirobenzopyran. Macromolecules 37, 4949–4955.
Sussman, E.M., Halpin, M.C., Muster, J., Moon, R.T., Ratner, B.D., 2014. Porous implants modulate healing and induce shifts in local macrophage polarization in the foreign body reaction. Ann. Biomed. Eng. 42, 1508–1516.
Szarowski, D.H., Andersen, M.D., Retterer, S., Spence, A.J., Isaacson, M., Craighead, H.G., Turner, J.N., Shain, W., 2003. Brain responses to micro-machined silicon devices. Brain Res. 983, 23–35.
Tanaka, T., Fillmore, D., Sun, S.-T., Nishio, I., Swislow, G., Shah, A., 1980. Phase Trans. Ion. Gels. Phys. Rev. Lett. 45, 1636–1639.
Tang, J., Xiao, P., 2009. Polymerizing immobilization of acrylamide-modified nucleic acids and its application. Biosens. Bioelectron. 24, 1817–1824.
Theodor, M., Ruh, D., Fiala, J., Forster, K., Heilmann, C., Manoli, Y., Beyersdorf, F., Zappe, H., Seifert, A., 2013. Subcutaneous blood pressure monitoring with an implantable optical sensor. Biomed. Microdevices 15, 811–820.
Thomé-Duret, V., Gangnerau, M.N., Zhang, Y., Wilson, G.S., Reach, G., 1996. Modification of the sensitivity of glucose sensor implanted into subcutaneous tissue. Diab. Metab. 22, 174–178.
Tien, H.-W., Lee, C.-Y., Lin, I.N., Chen, Y.-C., 2017. Long term in vivo functional stability and encapsulation reliability of using ultra-nanocrystalline diamond as an insulating coating layer for implantable microchips. J. Mater. Chem. B 5, 3706–3717.
Tilli, M., Motooka, T., Airaksinen, V.-M., Franssila, S., Paulasto-Kröckel, M., Lindroos, V., 2015. Handbook of Silicon Based MEMS Materials and Technologies, Micro Nano Technol. 2nd ed. Elsevier, pp. 787.
Toh, R.J., Mayorga-Martinez, C.C., Han, J., Sofer, Z., Pumera, M., 2017. Group 6 layered transition- metal dichalcogenides in lab-on-a- chip devices: 1T- phase WS 2 for microfluidics non- enzymatic detection of hydrogen peroxide. Anal. Chem. 89, 4978–4985.
U.S. Food & Drug Administration, 2015. Cybersecurity Vulnerabilities of Hospira Symbiq Infusion System: FDA Safety Communication. www.fda.gov/MedicalDevices/Safety/AlertsandNotices/ucm456815.htm. Accessed 18 August 2017. .
U.S. Food & Drug Administration, 2016a. The 670G System - P160017. www.fda.gov/MedicalDevices/ProductsandMedicalProcedures/DeviceApprovalsandClearances/Recently-ApprovedDevices/ucm522764.htm Accessed August 18, 2017. .
U.S. Food & Drug Administration, 2016b. Dexcom G5 Mobile Continuous Glucose Monitoring System - P120005/S041. www.fda.gov/MedicalDevices/ProductsandMedicalProcedures/DeviceApprovalsandClearances/Recently-ApprovedDevices/ucm533969.htm Accessed August 18, 2017. .

U.S. Food & Drug Administration, 2016c. Freestyle Libre Pro Flash Glucose Monitoring System. www.accessdata.fda.gov/scripts/cdrh/cfdocs/cfpma/pma_template.cfm?id=p150021 Accessed August 18, 2017. .

U.S. Food & Drug Administration, 2017. FDA Approves Pill With Sensor That Digitally Tracks If Patients Have Ingested Their Medication. www.fda.gov/NewsEvents/Newsroom/PressAnnouncements/ucm584933.htm Accessed November 28, 2017. .

Vaddiraju, S., Wang, Y., Qiang, L., Burgess, D.J., Papadimitrakopoulos, F., 2012. Microsphere erosion in outer hydrogel membranes creating macroscopic porosity to counter biofouling-induced sensor degradation. Anal. Chem. 84, 8837–8845.

Vallejo-Heligon, S.G., Brown, N.L., Reichert, W.M., Klitzman, B., 2016. Porous, Dexamethasone-loaded polyurethane coatings extend performance window of implantable glucose sensors in vivo. Acta Biomater. 30, 106–115.

Voskerician, G., Shive, M.S., Shawgo, R.S., Recum, Hv., Anderson, J.M., Cima, M.J., Langer, R., 2003. Biocompatibility and biofouling of MEMS drug delivery devices. Biomaterials 24, 1959–1967.

Wang, A., McAllister, J.P., Finlayson, P., Li, J., Brabant, K., Tang, H., Black, C., Cao, T., Liang, X., Salley, S.O., Auner, G.W., Ng, K.Y.S., 2007. Short-and long-term neural biocompatibility of heparin coated sapphire implants. Mater. Sci. Eng. C 27, 237–243.

Wang, B., Yoshida, K., Sato, K., Anzai, J.-i., 2017a. Phenylboronic acid-functionalized layer-by-layer assemblies for biomedical applications. Polymers 9, 202.

Wang, D., Hu, Y., Liu, P., Luo, D., 2017b. Bioresponsive DNA hydrogels: beyond the conventional stimuli responsiveness. Acc. Chem. Res. 50, 733–739.

Wang, G., Han, R., Su, X., Li, Y., Xu, G., Luo, X., 2017c. Zwitterionic peptide anchored to conducting polymer PEDOT for the development of antifouling and ultrasensitive electrochemical DNA sensor. Biosens. Bioelectron. 92, 396–401.

Wang, Y., Papadimitrakopoulos, F., Burgess, D.J., 2013. Polymeric "smart" coatings to prevent foreign body response to implantable biosensors. J. Control. Release 169, 341–347.

Wang, Y., Vaddiraju, S., Gu, B., Papadimitrakopoulos, F., Burgess, D.J., 2015. Foreign body reaction to implantable biosensors: effects of tissue trauma and implant size. J. Diabetes Sci. Technol. 9, 966–977.

Weir, R.F., Troyk, P.R., DeMichele, G.A., Kerns, D.A., Schorsch, J.F., Maas, H., 2009. Implantable myoelectric sensors (IMESs) for intramuscular electromyogram recording. IEEE Trans. Bio-Med. Eng. 56, 159–171.

World Health Organization, 2017. Diabetes Fact Sheet. www.who.int/mediacentre/factsheets/fs312/en/ Accessed August 31, 2017. .

Wilson, G.S., Gifford, R., 2005. Biosensors for real-time in vivo measurements. Biosens. Bioelectron. 20, 2388–2403.

Wisniewski, N.A., Klitzman, B., Miller, B., Reichert, W.M., 2001. Decreased analyte transport through implanted membranes: differentiation of biofouling from tissue effects. J. Biomed. Mater. Res. Part A 57, 513–521.

Wisniewski, N.A., Moussy, F., Reichert, W.M., 2000. Characterization of implantable biosensor membrane fouling. Fresen. J. Anal. Chem. 366, 611–621.

Worthington, K.S., Wiley, L.A., Mullins, R.F., Tucker, B.A., Nuxoll, E., 2016. Pre-vascularized silicon membranes for the enhancement of transport to implanted medical devices. J. Biomed. Mater. Res. B Appl. Biomater. 104, 1602–1609.

Xiao, X., Wang, J., Liu, C., Carlisle, J.A., Mech, B., Greenberg, R., Guven, D., Freda, R., Humayun, M.S., Weiland, J., Auciello, O., 2006. In vitro and in vivo evaluation of ultrananocrystalline diamond for coating of implantable retinal microchips. J. Biomed. Mater. Res. B Appl. Biomater. 77, 273–281.

Yoo, E.H., Lee, S.Y., 2010. Glucose biosensors: an overview of use in clinical practice. Sensors 10, 4558–4576.

Zhang, K., Huang, H., Yang, G., Shaw, J., Yip, C., Wu, X.Y., 2004. Characterization of nanostructure of stimuli-responsive polymeric composite membranes. Biomacromolecules 5, 1248–1255.

Zhang, L., Cao, Z., Bai, T., Carr, L., Ella-Menye, J.R., Irvin, C., Ratner, B.D., Jiang, S., 2013. Zwitterionic hydrogels implanted in mice resist the foreign-body reaction. Nat. Biotechnol. 31, 553–556.

Zhao, L., Wang, L., Zhang, Y., Xiao, S., Bi, F., Zhao, J., Gai, G., Ding, J., 2017. Glucose oxidase-based glucose-sensitive drug delivery for diabetes treatment. Polymers 9, 255.

Zhu, J., Wu, J., Tian, C., Wu, W., Zhang, H., Lu, D., Zhang, G., 1994. Microarray H2O2 electrodes as base elements of high-response glucose sensors. Sens. Actuators B: Chem. 20, 17–22.

Ziaie, B., Baldi, A., Lei, M., Gu, Y., Siegel, R., 2004. Hard and soft micromachining for BioMEMS: review of techniques and examples of applications in microfluidics and drug delivery. Adv. Drug Deliv. Rev. 56, 145–172.

Zourob, M., Ong, K.G., Zeng, K., Mouffouk, F., Grimes, C.A., 2007. A wireless magnetoelastic biosensor for the direct detection of organophosphorus pesticides. Analyst 132, 338–343.

Zschornack, E., Schmid, C., Pleus, S., Link, M., Klötzer, H.-M., Obermaier, K., Schoemaker, M., Strasser, M., Frisch, G., Schmelzeisen-Redeker, G., Haug, C., Freckmann, G., 2013. Evaluation of the performance of a novel system for continuous glucose monitoring. J. Diabetes Sci. Technol. 7, 815–823.